# SRI LANKAN GEOTECHNICAL SOCIETY

# ANNUAL CONFERENCE

30th September 2010

IESL Wimalasurendra Auditorium

**Welcome Message from the President, Sri Lankan Geotechnical Society**

The Sri Lankan Geotechnical Society (SLGS) formed in 1986 provides a forum for promoting cooperation among the engineers, geologists and other scientists in Sri Lanka for the advancement of knowledge in geotechnical engineering. Being a Member Society of the prestigious International Society of Soil Mechanics and Geotechnical Engineering (ISSMGE), we have been successful in getting cooperation also of the international community of geotechnical professionals in our efforts in sharing and disseminating geotechnical knowledge by way of conducting conferences, seminars, workshops, geotechnical forums and publishing journals and newsletters.

After a period of pestering terrorism that had virtually stalled development in Si Lanka well over three decades, we have entered a new era of rapid development. In the massive development projects that involve construction of roads, highways, railways, airports, harbours, bridges and multi-storied buildings and in the numerous rehabilitation, disaster mitigation & development programmes aimed at improving socio-economic conditions, services of our engineers and geotechnical professionals are indispensable and they have an important role to play. This is not limited to merely ensuring that foundations of structures are stable, safe and sound, but also involving in development activities by guiding the developers with proper geotechnical advice and inputs giving primary attention on the aspects of health, environment, sustainability and economy in every stage of planning, design and construction.

To take up the challenge, we need to broaden and update our knowledge in the science, techniques and practices in geotechnical engineering and the global and local experiences. We should be innovative to come up with new and appropriate technology, materials and equipment through research and application.

This year, giving emphasis to the young geotechnical engineers, the SLGS Annual Conference presents papers by four young members Mr. AJ Amerasinghe, Mr. KS Kahatadeniya, Dr. NH Priyankara and Mr. HR Madhuranga on innovative techniques and applications appropriate to local conditions. On behalf of the SLGS I sincerely welcome them and all the participants to this conference. I am hopeful that this forum will be a great opportunity for your interaction in sharing experiences and enhancing your knowledge. It will also encourage also the other members to publish and share their experiences among the geotechnical community through the SLGS.

Eng. Kirthi Sri Senanayake
President
Sri Lanka Geotechnical Society.

# SRI LANKAN GEOTECHNICAL SOCIETY

## EXECUTIVE COMMITTEE *for the term 2010*

| | |
|---|---|
| PRESIDENT | Eng. K.S. Senanayake |
| VICE PRESIDENT | Prof. S.A.S. Kulathilaka |
| PAST PRESIDENT | Prof. B.L. Tennekoon |
| PAST PRESIDENT | Eng. D.P. Mallawaratchie |
| HONY. SECRETARY | Eng. K.L.S. Sahabandu |
| ASST. SECRETARY | Eng. A.J. Amarasinghe |
| TREASURER | Eng.W.A.A.W. Bandara |
| ASST. TREASURER | Eng. R.M. Rathnasiri |
| EDITOR – JOURNAL | Dr. W. A. Karunawardena |
| EDITOR – NEWSLETTER | Dr. U.P. Nawagamuwa |
| COMMITTEE MEMBERS | Dr. N.H. Priyankara |
| | Dr. L.I.N. De Silva |
| | Ms. T.J.Jayasundara |
| | Mr. M.L.I. Abeysinghe |
| | Mr. H.R. Maduranga |

SECRETARIAT: National Building Research Organisation,
99/1, Jawatte Road,
Colombo 05.

# SLGS ANNUAL CONFERENCE, 2010

## PROGRAMME

| | |
|---|---|
| 1:00 - 1:20 | Registration |
| 1:20 - 2:20 | Presentation 1: **"Soil Nail Design Technique and its Application in the Repair of a Collapsed Rubble Masonry Wall"**<br>- *Eng. K L S Sahabandu* |
| 2:20 - 2:50 | Presentation 2: **"ANT Colony Optimization for Slope Stability Analysis"**<br>- *Mr. K S Kahatadeniya* |
| 2:50 - 3:00 | Discussion |
| 3:00 - 3:30 | Presentation 3: **"Suitability of Quarry Dust in Geotechnical Applications to Improve Engineering Properties"**<br>- *Dr N H Priyankara* |
| 3:30 - 4:00 | Presentation 4: **"Design of Surface and Sub surface Drainage Systems for Johnston Estate Resettlement Site, Nuwaraeliya using GIS Techniques"**<br>- *Mr. H R Maduranga* |
| 4:00 - 4:15 | Discussion and Concluding Remarks |
| 4:15 - 4:30 | Tea |
| 4:30 - 6:00 | 14th Annual General Meeting of the SLGS (for members only) |

*With Best Compliments from*

**ENGINEERS & ARCHITECTS cecb**

# SOIL NAILING UNIT
# CENTRAL ENGINEERING CONSULTANCY BUREAU


Head Office
No. 415, Bauddhaloka Mawatha, Colombo -07, Sri Lanka
Tel : +94 011-266-8800
Fax : +94 011-266-8956
E-mail : dec@cecbsl.com
Web : www.cecbsl.com

Contact Persons
Construction : Eng. Ranjan Kumara (DGM - Sabaragamuwa)
Tel : +94 - 45 222-6964
Fax : +94 - 45 222-6766

Design : Eng. Asanka Amarasinghe,
Tel : +94 - 11 2668829
Fax : +94 - 11 2668956


## DESIGN & CONSTRUCTION OF SOIL NAILING PROJECTS

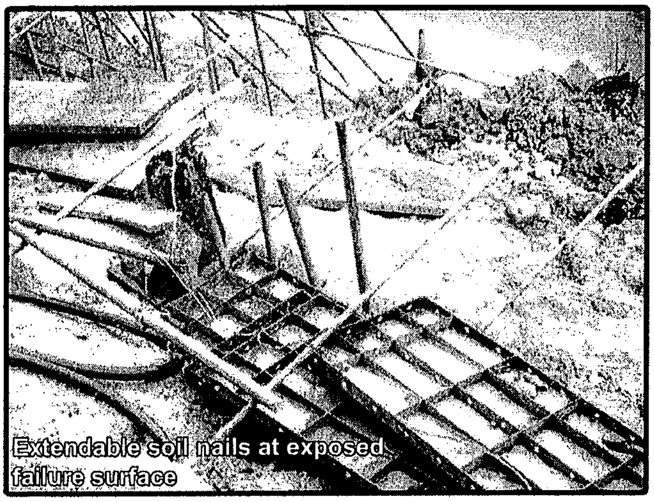

Extendable soil nails at exposed failure surface

Repair of collapsed rubble masonry retaining wall - diagrammatic section

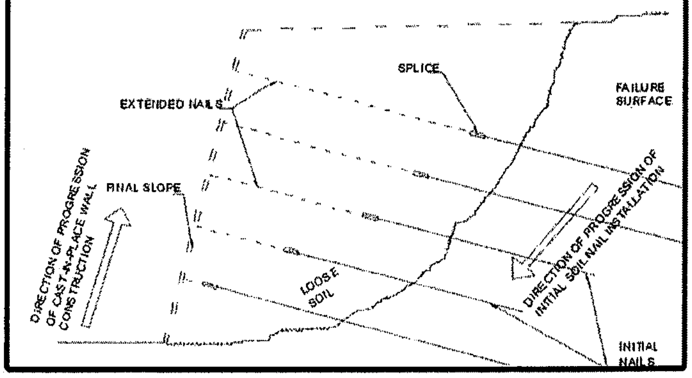


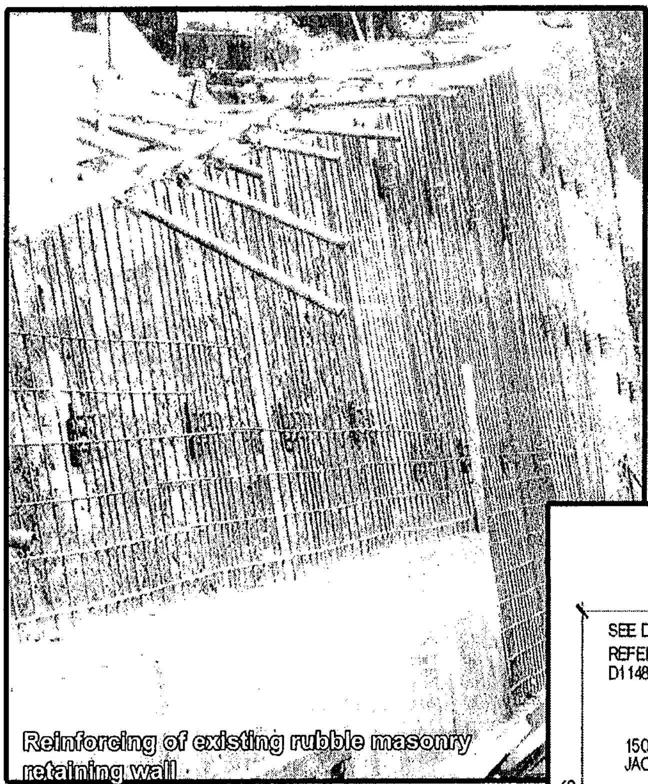

Reinforcing of existing rubble masonry retaining wall

### SOIL NAILING PROJECTS IN PROGRESS

1. **Repair of collapsed rubble masonry retaining wall at Kiriella police station using soil nailing technology.**
   **Area of soil nail wall - 348 sq.m**

2. **Soil nail wall at Kuruwita police station.**
   **Area of wall - 591 sq.m.**

3. **Soil nail wall at Rathnapura hospital.**
   **Area of wall - 333 sq.m.**

4. **Slope stabilation adjoining Swan Pond at Zoological Gardens, Dehiwala.**
   **Area of wall - 120 sq.m.**

Reinforcing of existing rubble masonry retaining wall - diagrammatic section

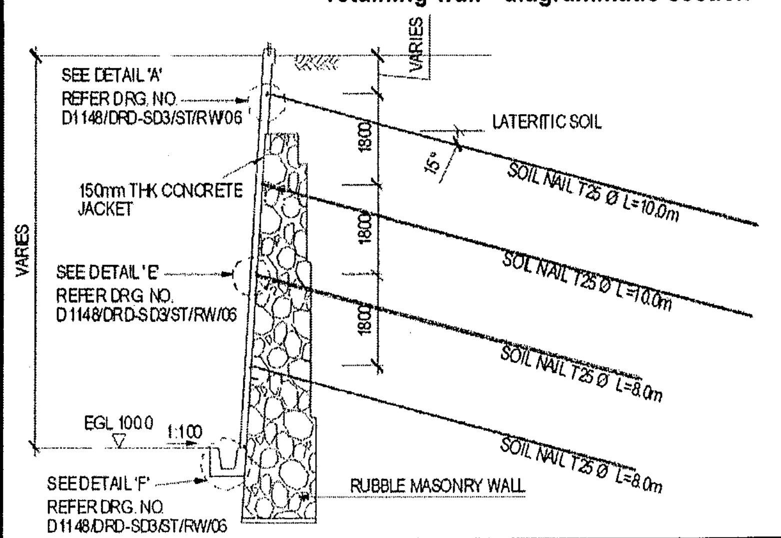


### SERVICES INCLUDE

- Soil investigations
- Preliminary Design
- Detail Design
- Cost Estimation
- Tender Documantation
- Construction
- Supervision

# CONTENTS

# Soil Nail Design Technique and its use in the Repair of a Collapsed Rubble Masonry Retaining Wall

SAHABANDU, K.L.S., AMARASINGHE, A.J.,
SANDARUWAN, H.J.K.G., PERERA, R.N.

Designs, Research and Development Section, Central Engineering Consultancy Bureau (CECB)

**ABSTRACT:** Soil nailing is a somewhat recent technique of stabilizing soil slopes, where slender elements of relatively high tensile capacity and low flexural rigidity, usually steel bars, are inserted into drilled holes and grouted. It is now an established technique in many parts of the world, owing to its many advantages over other methods such as gravity retaining walls, sheet pile walls, and Geo-grids. However, it is still in the process of gradually gaining popularity in Sri Lanka. This paper gives an introduction to the typical technique of soil nailing and the design process adhered to by the Federal Highway Authority of USA. It demonstrates that the use of the soil nailing technology is not restricted to general applications alone, by outlining an actual example of how a collapsed rubble masonry wall in Kiriella, adjoining the Panadura - Rathnapura road, was repaired using soil nailing. The unique nature of the problem demanded a non-standard construction technique and a different design methodology.

## 1. INTRODUCTION

The basic concept of soil nailing is to strengthen existing ground by installing closely spaced nails into a slope, thereby stabilizing the reinforced soil while effectively retaining the ground behind it. The reinforcing action is through nail-ground interaction. Although the nails are capable of resisting some amount of shear, it is generally conservative to ignore this in the design procedure, and to consider only their tensile capacity. In a frictional soil the effect of soil nailing is to improve stability by increasing the normal force and hence the shear resistance of soil along the potential failure plane. Even in cohesive soil types, it serves in reducing the driving force along the potential slip surface.

Typical soil nail walls have several advantages compared with conventional earth retaining systems particularly in excavation cuts. They offer improved economy and lessened environmental impact since there is no need for cut and backfill. Also, it is convenient since the temporary and permanent excavation support systems are incorporated into each other, and close nail spacing negates the need for a high capacity structural facing. Further, the elimination of cramped excavations cluttered with internal bracing leads to safer construction. Construction flexibility is a notable advantage where heterogeneous soils are present, overhead access is limited, and where difficult excavation shapes need to be accommodated. Soil nail walls are also quite robust and able to withstand considerable differential settlements.

Nevertheless, the soil nailing method also has a few limitations. Soil nails may have to be installed through land owned by an external party. In addition, problems may arise when encountering underground utilities, which could also pose the threat of inducing weakness along potential failure planes. Horizontal displacements may also be significant, causing possible distortion to nearby structures. The soil subject to nailing should exhibit a minimum degree of cohesion to facilitate an unsupported cut of up to 2m height, and should have a dewatered excavation face, in order to receive the shotcrete, or concrete facing.

The following is the typical construction sequence used for soil nail walls using drill and grout method of nail installation, which is the most common method used in North America.

i. Excavation of initial lift, to a depth slightly below the first row of nails, as is permitted by the ability of the soil face to stand on its own.

ii. Drilling of nail hole to a specified depth and angle.

iii. Installation and grouting of nails.

iv. Placing of drainage system.

v. Placing of construction facing and installation of bearing plates.

vi. Repetition of the process until the final elevation is reached.

vii. Placing of final facing.

## 2. DESIGN PHILOSOPHY

The fundamental mechanism of soil nailing structures is the utilisation of the tensile capacity of the reinforcement to support the stresses and strains within the soil which would otherwise cause the slope to fail. Soil nail loads develop primarily as a result of the skin friction between the soil and the grouted nail, and secondarily due to the soil–structure interaction between the facing and the soil slope. The active soil pressure acting on the facing of the soil nail wall is transferred to the nail head as a tensile force, which increases along the nail as the distance from the nail head increases. This is attributed to the skin friction acting in the outward direction along the nail within the "active" zone that lies within the failure wedge. The nail tension starts reducing however, after reaching the "resistant" zone, since the skin friction acts backwards along the nail from that point onwards.

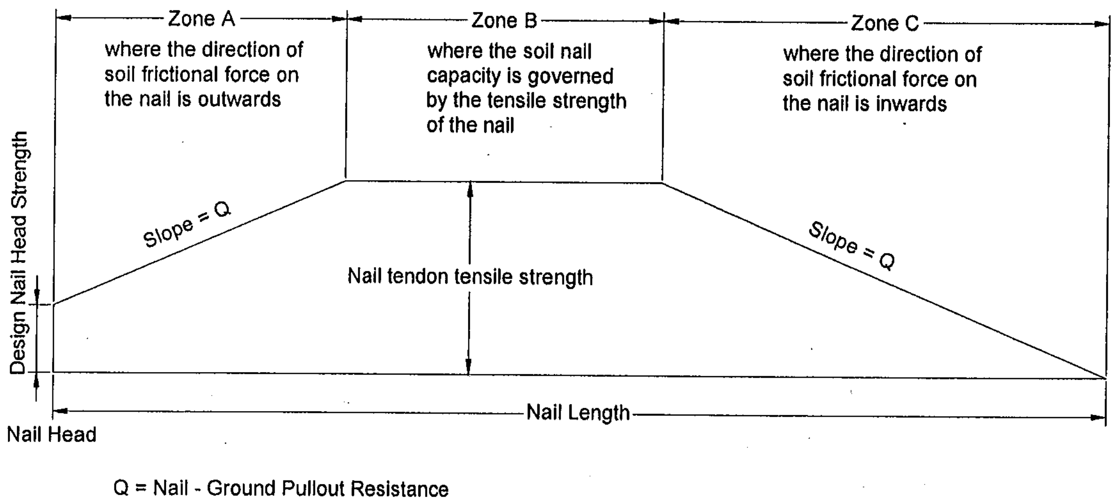


**Figure 1 – Nail support diagram**

The reinforcement therefore acts as a tie between the resistant zone and the active zone, which would otherwise fail by moving outwards and downwards with respect to the resistant zone. It follows that in order to achieve stability, three criteria need to be broadly satisfied, as illustrated by Fig. 2;

i. The tensile strength of the nail needs to be sufficient to resist the forces attempting to destabilize the active block.

ii. The nail needs to be embedded in the resistant zone up to a length sufficient for the required skin friction to develop in order to avoid pullout.

iii. The combined effect of the nail head capacity and pullout resistance of the length of nail between the face and the slip surface should be adequate to provide the required nail tension at the slip surface.

## 3. DESIGN PROCESS

The Manual for Design and Construction Monitoring of Soil Nail Walls, (FHWA 1996) describes two main design approaches for soil nail walls in detail. One of them is known as Service Load Design (SLD) while the other, which is adopted in this case study, is Load and Resistance Factor Design (LRFD). LRFD considers the strength limit state by ensuring that the factored design strength of the nails and the soil exceeds the applied loads, multiplied by load factors that are appropriate to their associated uncertainties.

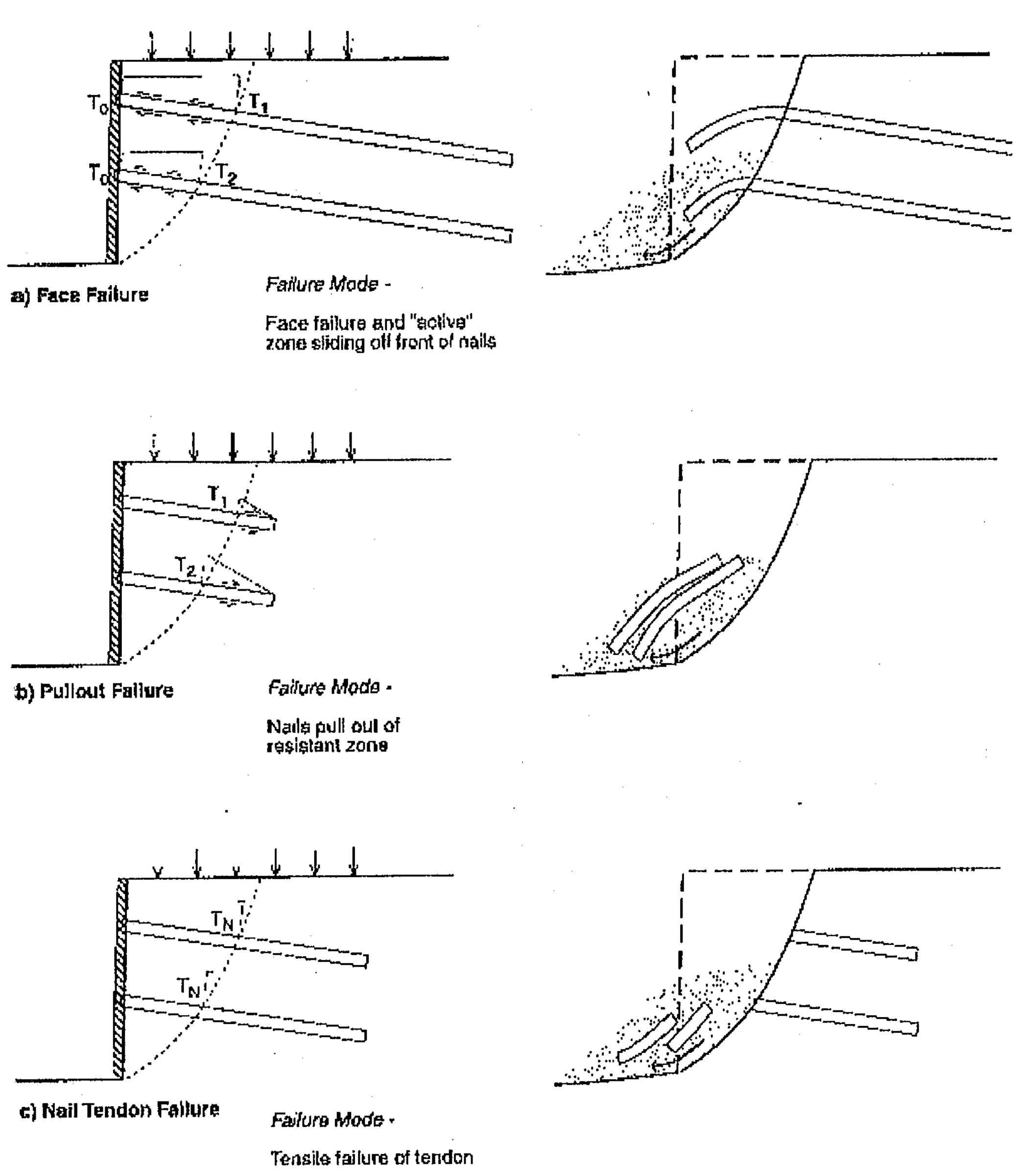


**Figure 2 – Potential soil nail wall failure mechanisms**

| ELEMENT | RESISTANCE FACTOR (STRENGTH LIMIT STATES) | RESISTANCE FACTOR (EXTREME LIMIT STATES) (SEISMIC) |
|---|---|---|
| Nail Head Strength | $\Phi_F$ dependent on failure mode | |
| Nail Tendon Tensile Strength | $\Phi_N$=0.90 | 1.0 |
| Ground-Grout Pullout Resistance | $\Phi_Q$ = 0.70 | 0.8 |
| Soil Cohesion | $\Phi_C$ = 0.90(0.90*) | 1.0(1.0*) |
| Soil Friction | $\Phi_\phi$ = 0.75(0.65*) | 1.0(0.9*) |
| Soil Cohesion-Temporary Construction Condition | $\Phi_C$ = 1.00(1.00*) | NA |
| Soil Friction – Temporary Construction Conditions | $\Phi_\phi$ = 0.85(0.75*) | NA |

*Soil strength resistance factors for "Critical "structures.

**Table 1 – Resistance factors - LRFD**

| Type of Load | Maximum Load Factor | Minimum Load Factor |
|---|---|---|
| DC | 1.25 | 0.90 |
| DW | 1.50 | 0.65 |
| EH<br>Active<br>At-Rest | <br>1.50<br>1.35 | <br>0.90<br>0.90 |
| EV<br>Overall Stability<br>Retaining Structures | <br>1.35<br>1.35 | <br>N/A<br>1.00 |
| ES | 1.50 | 0.75 |

Where,
DC = Dead load of structural components and non-structural attachments.
DW = Dead load of wearing surfaces and utilities.
EH = Horizontal earth pressure load.
EV = Vertical pressure from dead load of earth fill.
ES = Earth surcharge load

**Table 2 – Load factors for permanent loads – LRFD**

The design process is carried out in accordance with steps as follows;

STEP 1 – Set up critical design cross section and select a trial design

The preliminary design charts shown in Figs. 3 and 4 are used to determine the preliminary values for nail length and nail bar size.

The dimensionless nail tensile capacity, $T_D$ can be obtained from Fig. 3 using the factored soil friction angle and factored cohesion. Once $T_D$ has been obtained, it can be used to compute $T_{NN}$, the required nominal nail strength, through the equation,

$T_D = \Phi_N T_{NN} / (T_W \gamma H S_V S_H)$, where $\Phi_N$ is the nail tendon tensile strength factor, $S_V$ and $S_H$ are the vertical and horizontal nail spacings respectively, and the remaining terms are as given in Fig. 3.

The next step is to calculate the dimensionless nail pullout resistance, $Q_D$, given by

$Q_D = \Phi_Q Q_U / (T_W \gamma S_V S_H)$ where $\Phi_Q$ is the ground-ground pullout resistance factor, and $Q_U$ is the ultimate pullout resistance.

This enables the computation of $T_D/Q_D$, which in turn is used in the chart in Fig. 4 to calculate the preliminary nail length, L

STEP 2 – Determine the Allowable Nail Head Loads

The determination of nail head strength investigates three critical failure mechanisms for the failure of the soil nail wall facing as well as the connection system, which are given in Figure 2;

i. The shotcrete / concrete face / wall may fail in flexure.

ii. The shotcrete / concrete face / wall may fail in punching shear.

iii. The headed stud may fail in tension.

STEP 2.1 – Strength Criteria i : Fail in Flexure

In order to provide flexural strength to the concrete or shotcrete wall, a steel reinforcement net is often used at midsection throughout the full area of the wall. Providing the reinforcement at midsection ensures maximum cover and also enables the section to resist both hogging as well as sagging moments. Two or more vertical bearing bars are also provided at nail head locations for additional resistance to hogging moments. Along with the horizontal waler bars placed behind the bearing plates continuously across, they also serve in achieving development of full plastic moments in the slab. The waler bars also contribute to the ductility of the slab in case of punching shear failure.

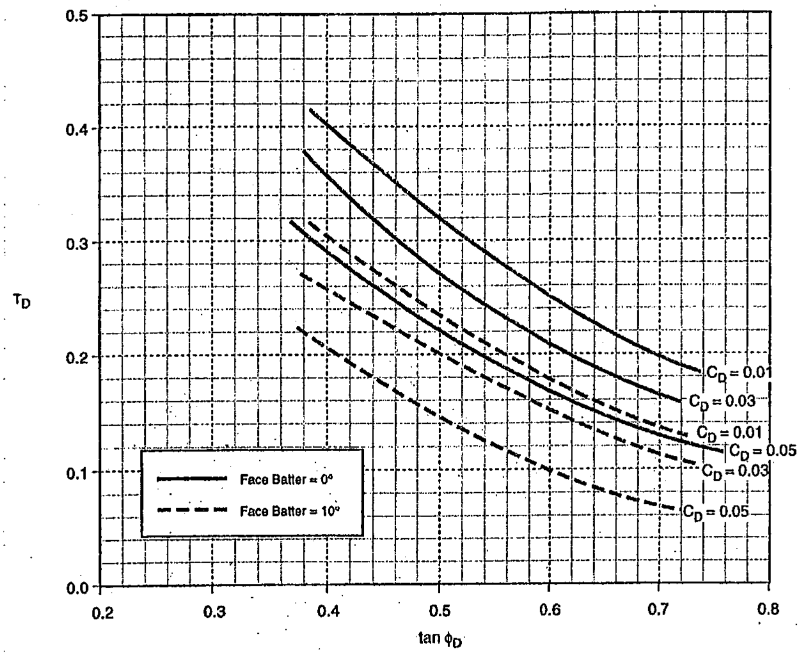


$\phi_D = \tan^{-1}[\Phi_\Phi \tan(\phi_U)]$, where,

$\phi_U$ = ultimate soil friction angle
$\phi_D$ = factored soil friction angle
$\Phi_\Phi$ = soil friction resistance factor (see Table 1)

$C_D = \Phi_C C_U / (T_W \gamma H)$, where,

$C_D$ = dimensionless cohesion
$C_U$ = ultimate soil cohesion
$T_W$ = load factor for soil weight (see Table 2)
$\gamma$ = unit weight of soil
H = vertical height of soil nail wall
$\Phi_C$ = soil cohesion resistance factor (see Table 1)

**Figure 3 – Preliminary design chart for back slope of 20° (Typical)**

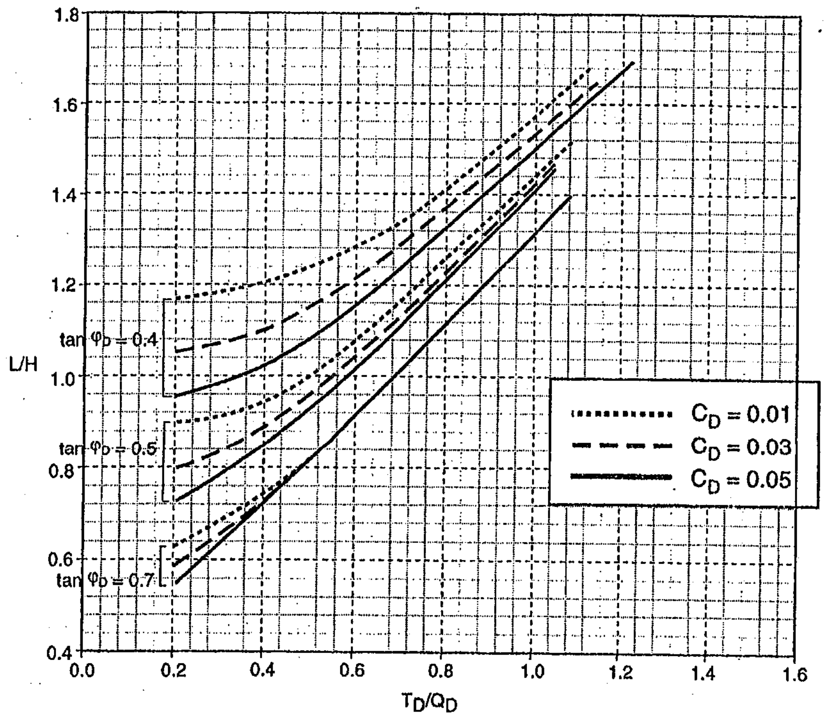


**Figure 4 – Preliminary design chart for face batter 10° and back slope 20° (Typical)**

The capacity of the nail head in terms of resistance of the facing to flexure has been found to be represented by;

$$T_{FN} = C_F(m_{v,neg}+m_{v,pos})(8)(S_H)/(S_V)$$

Where, $C_F$ is a facing flexure pressure factor, $S_H$ and $S_V$ are the nail spacings in horizontal and vertical directions, and $m_v$ is the unit moment of resistance for hogging or sagging moments, given by;

$$m = \frac{A_s F_Y}{b}\left(d - \frac{A_s F_Y}{1.70 f'_c b}\right)$$

Where; m = nominal unit moment resistance of the facing

$A_S$ = area of tension reinforcement of facing panel width 'b'

$F_Y$ = tensile yield stress of reinforcement

b = width of unit facing panel, equal to $S_H$

d = distance from extreme compression fibre to centroid of tension reinforcement

$f'_C$ = concrete compressive strength

STEP 2.2 – Strength Criteria ii : Fail in Punching Shear

The nail head strength for resisting punching shear of the facing in bearing plate connections is given by;

$$T_{FN} = V_N\left(\frac{1}{1 - C_S(A_C - A_{GC})/(S_V S_H - A_{GC})}\right)$$

Where, $A_C$ is the area of punching shear cone base at the back of the facing, while $A_{GC}$ is the cross sectional area of the grout column and $C_S$ is the pressure factor for punching shear. The equation is derived by considering the equilibrium between the following 3 forces;

i. $V_N$, the nominal internal punching shear strength of the facing, given by;

$$V_N = 0.33\sqrt{f'_C\,(MPa)}\,(\pi)(D'_C)(h_C)$$

Where, $D'_C$ = the effective diameter of the punching shear cone,

$h_C$ = the effective height of the punching shear cone,

$f'_C$ = the concrete compressive strength.

ii. The tensile force applied by the soil nail on the punching shear cone, also equal to $T_{FN}$ at limiting conditions.

iii. The soil pressure acting at the base of the punching shear cone. This is based on the average pressure acting on the influence area of the soil nail, $T_{FN}$ / ($s_V$ $s_H$ - $A_{GC}$), which is multiplied by the area of soil supporting the punching cone, and a factor $C_S$ to account for the increase of pressure closer to the vicinity of the nail.

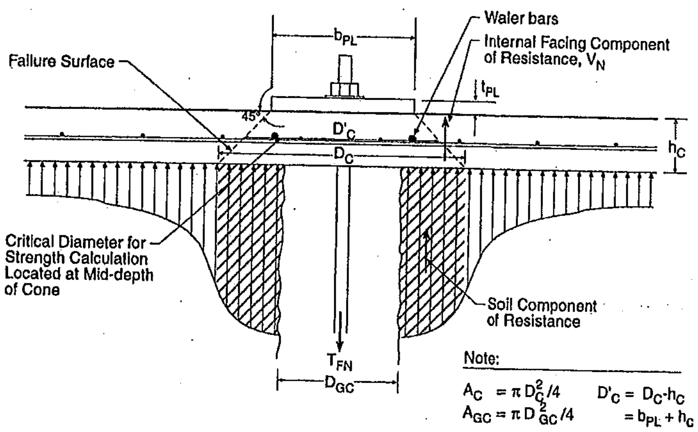


**Figure 5 – Punching shear in a temporary bearing plate connection**

Where a headed stud arrangement is present, as is the case when a cast-in-place permanent facing is applied on the shotcrete facing, the punching shear cone is assumed to extend from the top of each headed stud.

STEP 2.3 – Strength Criteria iii: Nail Stud Fail in Tension

The computation of nail head capacity in terms of nail stud tension is straightforward, based on the characteristic strength of the stud material, and the cross sectional area of the stud. For a nail head with 4 headed studs;

$$T_{FN} = 4 A_{HS} F_U$$

Where, $A_{HS}$ is the cross sectional area of the body of the headed stud, and $F_U$ is its ultimate tensile strength.

STEP 3 – Minimum design nail head strength check

Once the minimum nominal nail head strength is computed using the criteria of flexure, punching shear and nail head stud tension, it is compared, applying an appropriate factor of safety, with the force on the nail arising from the active pressure acting around each nail. This force is given by;

$$t_F = F_F K_A \gamma H S_H S_V$$

Where, the active pressure coefficient $K_A$ is obtained from Coulomb Theory, and $F_F$ is the nail head service load factor, usually assumed to be 0.5. H is the vertical height of the soil nail wall.

STEP 4 – Define the design nail head strength diagram

Here, the parameters required to draw the diagram given in Fig. 1 are computed as follows;

$T_F$ (Design nail head strength) = lesser of the nail head strengths obtained from steps 2.1, 2.2, and 2.3 above.

Q (Design pullout resistance) = $\Phi_Q Q_U$ (terms defined above)

T (Design nail tendon tensile strength) = $\Phi_N T_{NN}$ (terms defined above)

STEP 5 – Select trial nail spacings and lengths

Fig. 6 gives the procedure to be followed in obtaining the trial nail profile. Once the R value corresponding to $Q_D/(L/H)$ is read from the chart given in Fig. 6.2, the trial nail profile can be set as indicated.

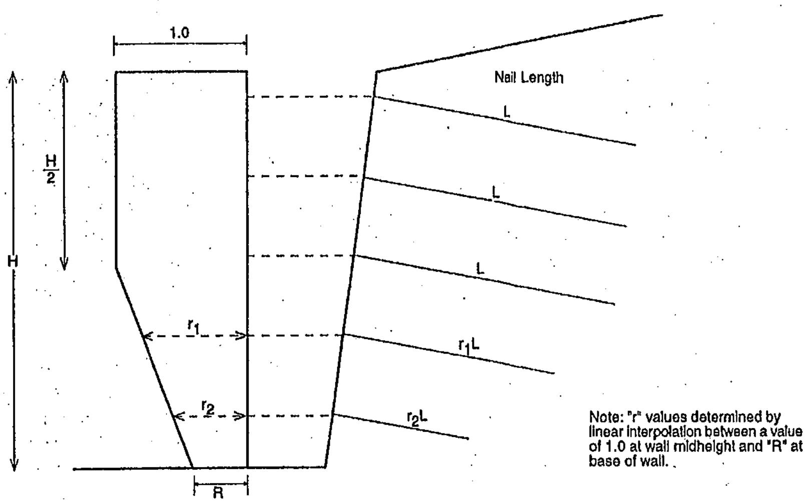


**Figure 6.1 – Nail length distribution assumed for design**

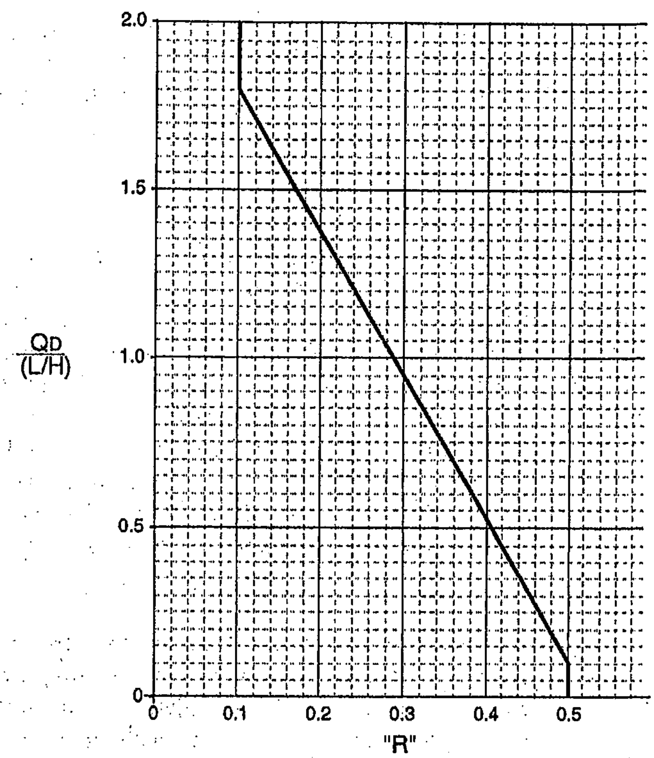


**Figure 6.2 – Derivation of "R"**

STEP 6 – Define the design soil strengths

Design angle of friction as well as cohesion are derived as follows;

$\phi = \tan^{-1}[\Phi_\Phi \tan(\phi_U)]$

$c = \Phi_C c_U$ (terms defined above)

STEP 7 – Calculate the Load/Resistance ratio

Once the nail head capacity is found to be satisfactory for the given nailing arrangement, the stability of the slope is checked using a computer software which uses a method of slices such as Bishop's, Janbu's or Morgenstein-Price's. The software that was used in this case study models the slope using soil strength parameters, nail properties, nail and slope geometry, loading etc. inputted by the user. Internally, the program calculates Factors of Safety for multiple predefined circular slip surfaces and lists them in order of magnitude. A trial and error process is used, changing various parameters such as nail length and nail angle, to arrive at the optimum nailing arrangement.

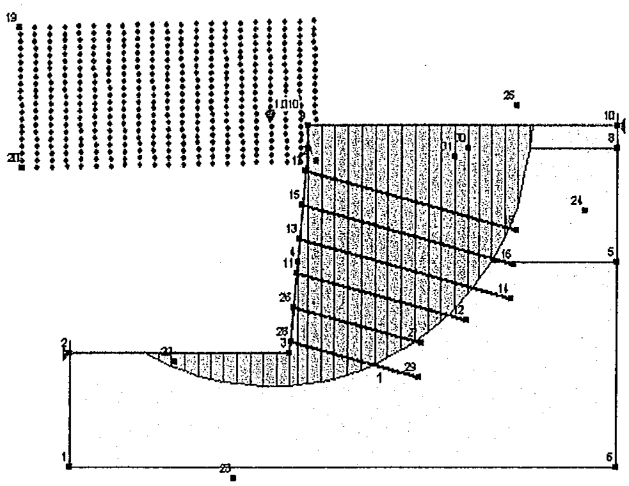

**Figure 7 – Computer output for analysis of soil nail wall (Typical)**

Unless the above computer analysis is performed by a software package that has been thoroughly verified for accuracy, it is advisable to perform a manual check on the final arrangement once the nail loads are known. An example of a simplified check is given in Figure 3.3.

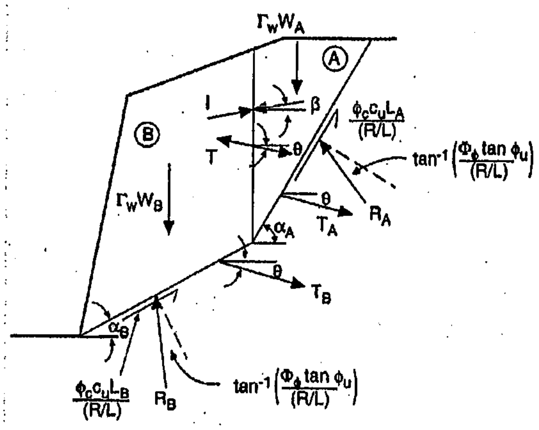


**Figure 8 – Manual check of computer software results**

From the above diagram, four equations can be written for the horizontal and vertical equilibrium of each wedge, the only unknowns being R/L (Resistance/Load=F.O.S), $R_A$, $R_B$ and I. β may be assumed to be equal to zero;

Define $\phi = \tan^{-1}[\tan(\phi_U)/F]$.

<u>Block A</u>

<u>Vertical</u>

$$W_A + (T_A - T)\sin(\theta) - (I)\sin(\beta) - c_U(L_A)\sin(\alpha_A)/F - (R_A)\cos(\alpha_A - \phi) = 0$$

<u>Horizontal</u>

$$(I)\cos(\beta) + (T_A - T)\cos(\theta) + c_U(L_A)\cos(\alpha_A)/F - (R_A)\sin(\alpha_A - \phi) = 0$$

<u>Block B</u>

<u>Vertical</u>

$$W_B + (T_B + T)\sin(\theta) + (I)\sin(\beta) - c_U(L_B)\sin(\alpha_B)/F - (R_B)\cos(\alpha_B - \phi) = 0$$

<u>Horizontal</u>

$$(I)\cos(\beta) - (T_B + T)\cos(\theta) - c_U(L_B)\cos(\alpha_B)/F + (R_B)\sin(\alpha_B - \phi) = 0$$

In addition to carrying out the above procedures, a complete design also requires that checks be made to ensure external stability of the nail block and the stability of the upper cantilever. Further, detailing aspects should be given due attention, for both for the shotcrete and concrete facing reinforcement. Also, for the permanent facing of the upper cantilever, a serviceability check must be carried out to ensure that steel is not overstressed.

## 4. CASE STUDY

The following case study is an example of how the soil nailing design and construction technique generalised above was modified and adapted to suit a practical situation which arose in Kiriella, in the Rathnapura District. Rathnapura has an annual rainfall which is among the highest in the country, averaging between 4000 and 5000mm. Since the region is also hilly, landslides are an ever present threat.

The site is situated next to the Panadura-Rathnapura road on an approximately 100m long strip of land created by cutting into the existing slope, building a retaining wall and backfilling up to the desired finish level. The retaining wall varies in height starting from approximately 3m to approximately 10m at its highest, measured from road finish level.

Attention was drawn to the site as a result of collapse of a sizeable portion of the existing retaining wall which occurred during the rainy season, endangering the newly constructed building above the retaining wall.

Investigations into the underlying reasons for the collapse showed that the existing gravity retaining wall offered very little safety against overturning. This was due to a faulty design, which had provided only a 1.5m wide base, grossly inadequate to retain a 9.5m height of soil. Although the retaining wall was constructed in wide panels within a reinforced concrete beam-column frame, there seemed to be no apparent basis for it. Also, the foundation was not wide enough to satisfy minimum stability criteria.

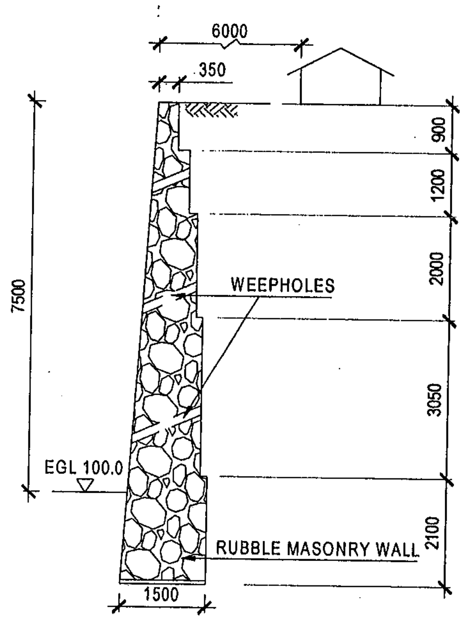


**Figure 9 – Sectional elevation of existing retaining wall at highest embankment elevation.**

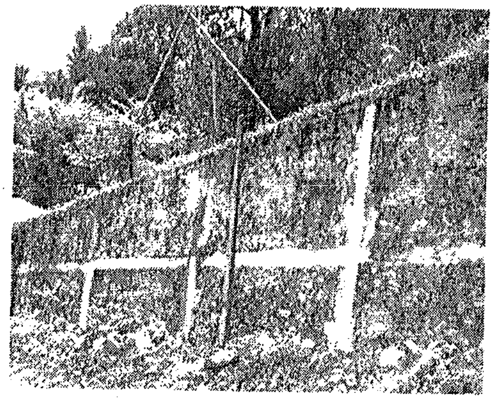

**Figure 10 – Frontal view of part of the unaffected rubble masonry retaining wall.**

As a solution to the above problem, the method adopting the proposed form of soil nailing, was chosen for the following reasons;

i. The need to avoid damages to buildings on top of the embankment due to further collapse.

ii. The cost saving achieved, by incorporating the existing retaining walls unaffected by the collapse, into the composite soil retaining arrangement.

iii. The elimination of the need to carry out large scale excavations for new gravity retaining wall foundations. This is most important due to the presence of both the existing building above the embankment as well as the public main road.

iv. The urgent need to avoid further collapse due to the prevailing frequency of rainfall, by adopting a methodology which could be implemented quickly.

The proposed method for remediation consisted of two main aspects;

a. The introduction of a retaining mechanism where the retaining wall section has been destroyed due to the collapse.

b. Reinforcing of the existing unaffected retaining wall.

4.1 Reinstatement of Slope at Collapsed Retaining Wall Section

The above repair is being carried out by adopting the following procedure;

i. Drilling of nail holes, insertion of nails and grouting of nail holes at locations projected from predefined points on proposed final face from the top of the collapsed slope progressing to the bottom.

ii. Careful removal of loose soil in the vicinity of the slip surface, advancement of concrete facing up to the level of the bottommost nail row, extension and grouting of the extended nails encased in PVC pipes.

iii. Backfilling of slope covering the newly extended and grouted nail and repeating the process from Step i. until top of slope is reached.

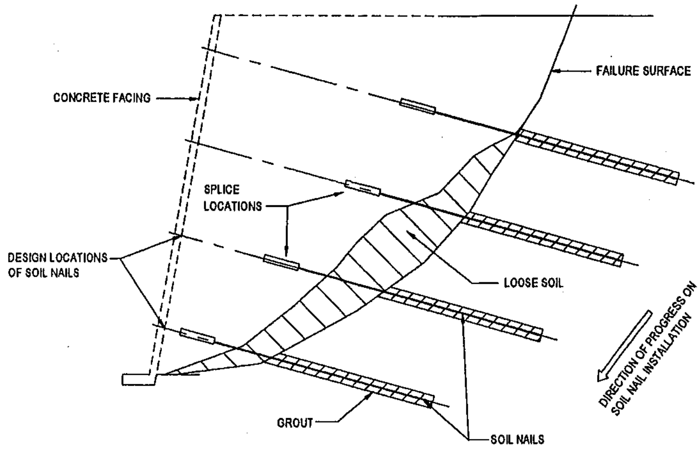


STAGE 1

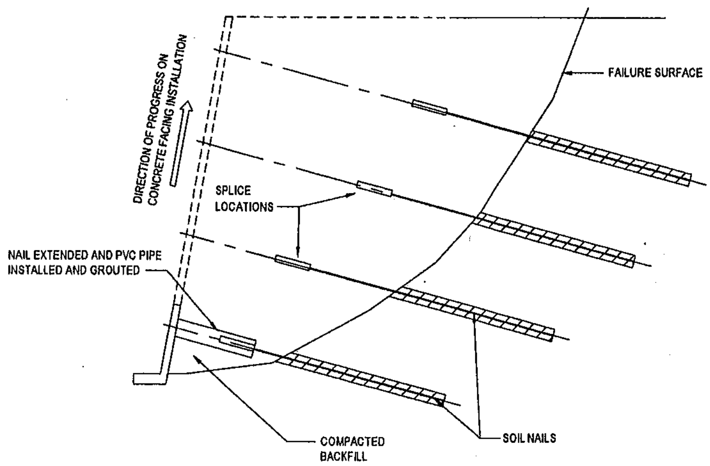


STAGE 2

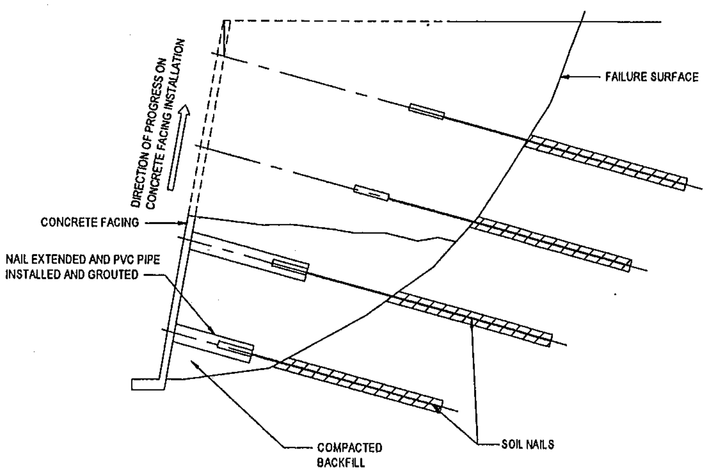


STAGE 3

**Figure 13 – Construction sequence for cast-in-place concrete wall and nail extensions**

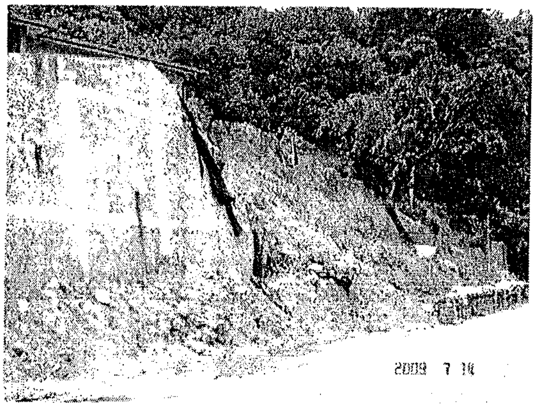

**Figure 11 – View of partially collapsed retaining wall prior to repair**

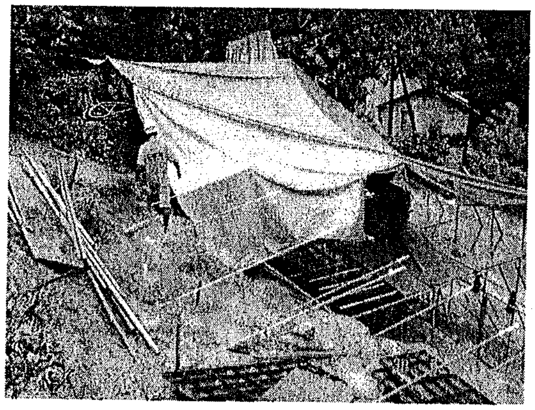

**Figure 12 – Extendable soil nails installed in the failed slope.**

The analysis of the problem was done in two stages. Observations made at site indicated that the current slope inclusive of loose soil and debris is in a stable state, in comparison to the much steeper original slope. However, it was necessary to check whether the removal of loose soil from the failed slope in order to proceed with the repair would result in further collapse. In order to do so, a stability analysis was carried out on the failed slope with soil nails installed. It should be emphasised here that although the absence of a facing may cause local failure in the vicinity of the failed soil surface, the slope would be protected against slip failure across the nailed soil. The arrangement is justified since the cohesion values obtained from triaxial tests in the region suggest that the soil is of adequate cohesion to resist a local failure of the slope face. Further, the bond between the nails and soil at the vicinity of the slipped surface provides better stability than that which would exist in the absence of nails.

Secondly, a stability analysis is carried out for the final slope, with the new facing and extended nails. Here, since the extended nail portion is encased in PVC tubing, which provides a lesser skin friction with the surrounding soil, the nail head should be capable of resisting the maximum tension that could develop in the nail.

4.2 Reinforcing of the Existing Unaffected Retaining Wall

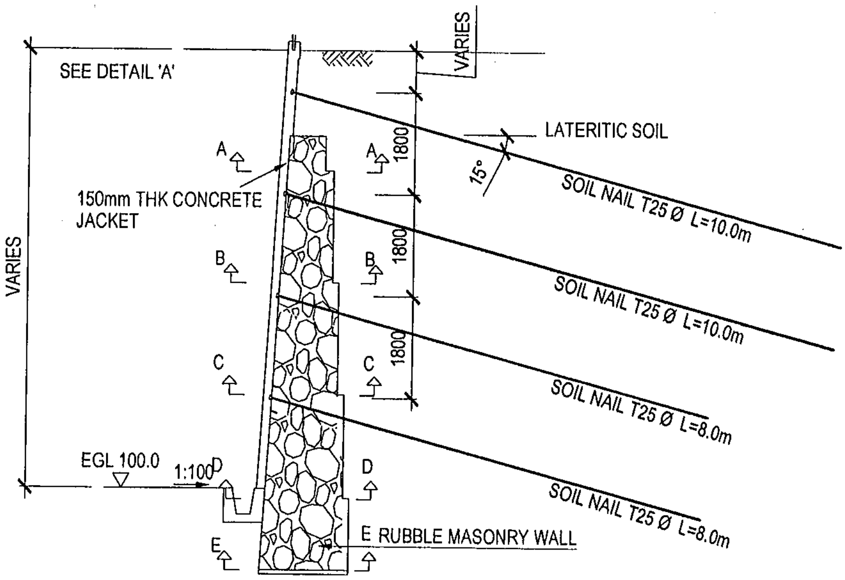

In this particular case the collapse of the rubble masonry wall exposed the inadequacy of the retaining wall section given the prevailing conditions, and strongly suggested that in order to avoid further collapse, it was necessary to strengthen the existing wall. Also, in comparison to constructing a new retaining wall, the proposed arrangement results in a considerable saving in cost.

Here too, the purpose of installing the nails is twofold. The first of these is the necessity to minimise the probability of deep seated failure. This is addressed by analysing the stability of the nailed slope. In doing so, the stabilising effect of the gravity retaining wall is ignored. However, this conservative assumption is acceptable since the collapse had already proven the wall's ineffectiveness. This was further justified when initial attempts to drill nail holes in the rubble wall revealed that the mortar used was of poor quality.

The other purpose is to directly provide stability to each block of the retaining wall via the mobilisation of nail tension, which would serve to provide a restoring moment against overturning outwards. Approximate values were assumed for the nail head tensile forces, and overturning checks were performed. In addition, the same analysis was used to demonstrate that each block was safely within allowable stresses, and that sliding of the foundation would not occur. A reinforced concrete jacketing on the outside of the rubble masonry wall was required to provide necessary tensile stress capacity due to the action of soil nail reaction.

| Section | Factor of Safety Against | | | | Stress on inner face (Compression(+)ve) $N/mm^2$ | | Stress on outer face (Compression(+)ve) $N/mm^2$ | |
|---|---|---|---|---|---|---|---|---|
| | Overturning | | Sliding | | | | | |
| | Before | After | Before | After | Before | After | Before | After |
| A – A | 2.46 | 8.88 | NA | NA | -0.05 | 0.13 | 0.14 | -0.04 |
| B – B | 0.72 | 5.03 | | | -0.25 | 0.85 | 0.43 | -0.67 |
| C – C | 0.31 | 2.87 | | | -1.05 | 1.77 | 1.33 | -1.49 |
| D – D | 0.24 | 2.30 | | | -1.76 | 2.06 | 2.12 | -1.70 |
| E – E | 0.21 | 1.89 | 0.514 | 2.150 | -2.57 | 1.89 | 2.97 | -1.49 |

**Table 3**
**Comparison between retaining wall without nails and retaining wall with nails for 8m high wall section**

## 5. CONCLUSION

Soil nail walls can be used to provide solutions to a variety of problems related to slope stability. The most common construction sequence adopts a top-down approach, where the final slope is achieved by cutting into the existing topography. However, the basic principles of soil nailing can be applied to situations which are more site-specific, which cannot be addressed by using the standard construction methods. The case study illustrated above, giving two different applications of soil nailing technique, is a typical example of such a situation.

Soil nailing design, as well as construction methods are numerous, and are not restricted to the soil nailing techniques described herein. Basic designs may differ with respect to type of facing used; method of subsurface drainage; the extent of shotcrete used, and so on, while there can also be a wide variation in construction methodology used. The basic principles however, remain the same, and can be used hand in hand with theoretical as well as practical engineering knowhow to provide innovative solutions to challenging problems encountered in the field. The above case studies for instance, demonstrate how the stability of an under-designed gravity retaining wall can be improved using soil nailing technology.

It could be concluded that in comparison with other earth retaining methods, soil nailing may very often be the most viable solution for overcoming certain construction challenges, and should not be ruled out as an option without careful consideration of the pros and cons involved.

## 6. REFERENCES

Byrne, R.J., Cotton, D., Porterfield, J., Wolschlag, C., Ueblacker, G., "Manual for Design and Construction Monitoring of Soil Nail Walls", Federal Highway Administration, U.S. Department of Transportation, 1998.

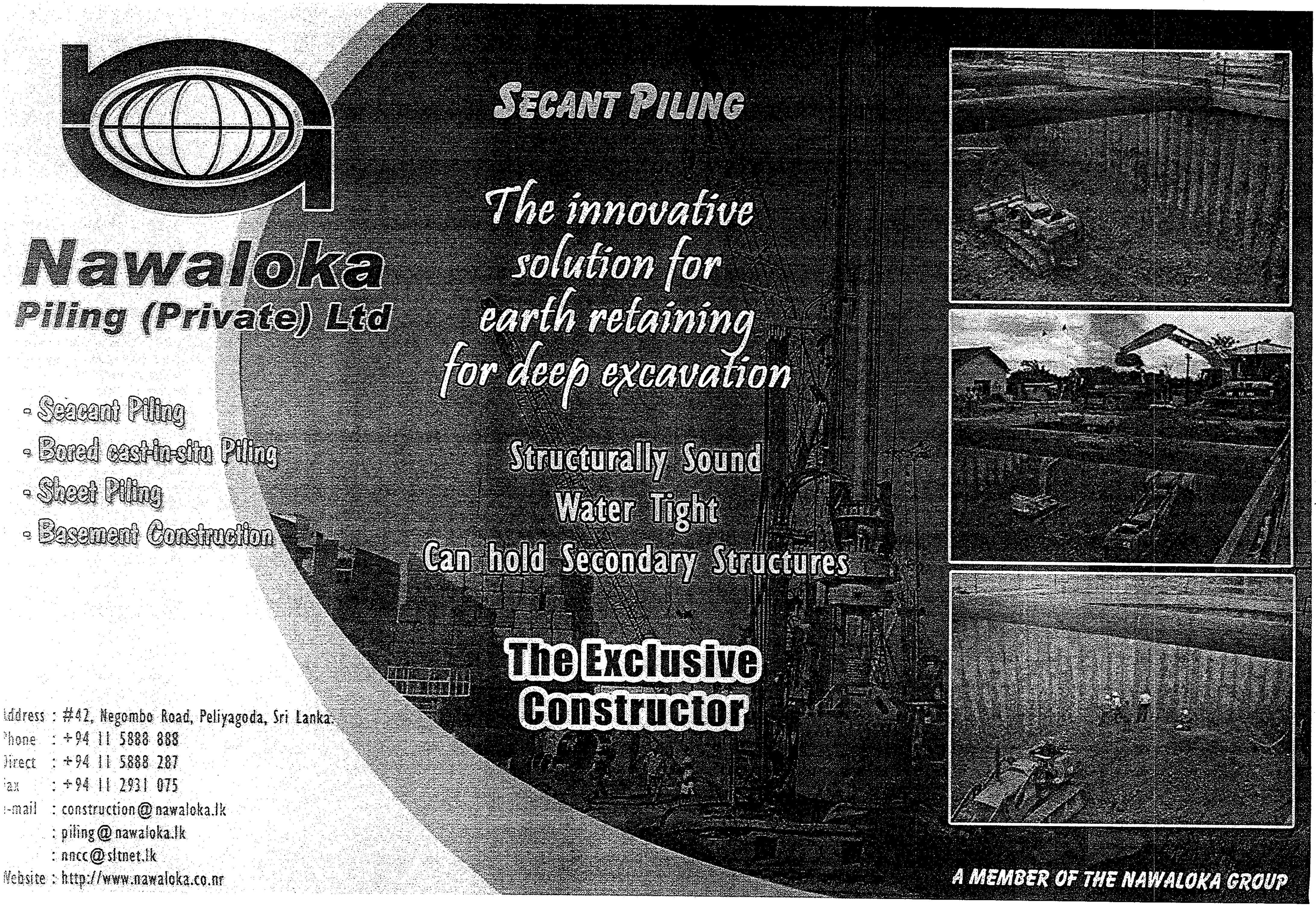
Nawaloka
Piling (Private) Ltd
Seacant Piling
Bored cast-in-situ Piling
Sheet Piling
Basement Construction
SECANT PILING
The innovative solution for earth retaining for deep excavation
Structurally Sound
Water Tight
Can hold Secondary Structures
The Exclusive Constructor
ddress : #42, Negombo Road, Peliyagoda, Sri Lanka.
hone : +94 11 5888 888
irect : +94 11 5888 287
ax : +94 11 2931 075
-mail : construction@nawaloka.lk
: piling@nawaloka.lk
: nncc@sltnet.lk
Vebsite : http://www.nawaloka.co.nr
A MEMBER OF THE NAWALOKA GROUP

# ANT COLONY OPTIMIZATION FOR SLOPE STABILITY ANALYSIS

**K. S. Kahatadeniya,** Oriental Consultants Company Ltd., Outer Circular Highway to the City of Colombo (OCH) Project, No.560/6,Udumulla Road, Battaramulla, Sri Lanka.

## Abstract

The analysis of slope stability that searches for the critical failure surface with the lowest factor of safety can be performed by numerical optimization techniques and several optimization methods have been used successfully. These methods include traditional mathematical optimization techniques as well as recently developed heuristic optimization techniques. In order to determine safety factors of different slip surfaces, various limit equilibrium methods, which are either based on force equilibrium or force and moment equilibrium of the inter-slice forces, have been always used. In this study, the ant colony optimization (ACO) method is used to identify the critical failure surface. The Morgenstern and Price method is employed to estimate safety factors of slip surfaces as it is considered mathematically rigorous. In addition, the Newton-Raphson method is used to solve the nonlinear equations obtained from the Morgenstern and Price method. In this study, uniformly distributed vertical overburden forces and pseudo-static earthquake forces are taken into account. The validity and efficiency of the proposed method is shown by solving problems from the literature.

**Key words**: Critical failure surface, Factor of safety, Ant colony optimization

## 1. Introduction

The aim of slope stability analysis of any natural or artificial slope is to determine the factor of safety of the slope. This task is possible only if the critical failure surface of the slope is accurately found or estimated. Obviously, the critical failure surface of a slope is the slip surface that possesses the lowest factor of safety. Traditionally, the critical failure surface is found by comparing safety factors of several trial slip surfaces. These safety factors are usually computed by using limit equilibrium methods that satisfy equilibrium conditions for a kinematically admissible failure soil mass. The limit equilibrium methods by Morgenstern and Price [1], Spencer [2], Bishop [3] and Janbu [4] are a few popular approaches. The trial and error method is clearly not the most efficient way to find the critical failure surface. Apparently, optimization methods can be employed. Many optimization approaches have been employed to automate the search for the critical failure surface. Examples include the dynamic programming by Baker [5] as well as Monte Carlo techniques by Malkawi et al. [6] and Greco [7]. Since the recent development of evolutionary algorithms, genetic algorithms (GAs) have also been successfully used to identify the critical slip surface by, for example, Goh [8], McCombie and Wilkinson [9], Das [10], Zolfarghari et al. [11], and Jianping et al. [12]. In addition to finding the critical failure surface, Zolfarghari et al. [11] also used the GA to approximately solve the limit equilibrium equations employed.

In this study an ACO approach is used to locate the critical slip surface. Safety factors of slip surfaces are found by using the Morgenstern and Price method, which satisfies both force and moment equilibrium simultaneously. Nonlinear equilibrium equations that arise from the Morgenstern and Price method are solved numerically using the Newton-Raphson method. In this way, the numerical strength of the Newton-Raphson method and the optimizing capability of the heuristic ACO technique are both effectively utilized. Also in the problem definition, pseudo-static horizontal and vertical forces due to an earthquake and a uniformly distributed vertical overburden force are included. There is no assumption made on the starting and ending points as well as the shapes of slip surfaces. The obtained results are compared with the existing results found in the literature.

## 2. Determination of the critical failure surface

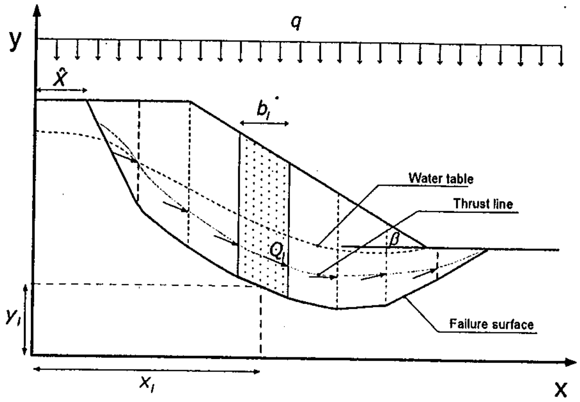


**Figure 1.** Typical sliding mass

Consider a typical slip surface of a general shape shown in Figure 1. In the figure, the potential sliding mass is divided into '$n$' vertical slices. Consider a typical $i^{th}$ slice shown in Figure 2. When the mass becomes unstable, the slice is subjected to typical forces also shown in the same figure. Note that, in this study, effective stress analysis is employed. The failing mass is moving from left to right. The angle of the base of the slice ($\alpha$) is always shifted counter-clockwise to make the slip surface admissible.

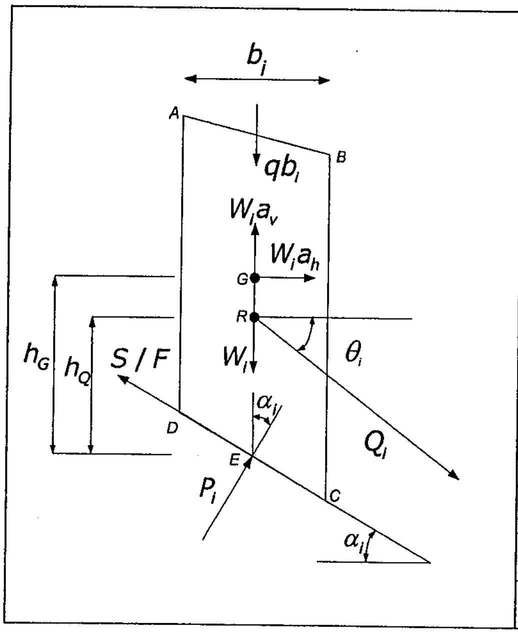


| | |
|---|---|
| $W_i$ | Weight of the $i^{th}$ slice |
| $a_v$ | Pseudo-static coefficient for vertical earthquake loading |
| $a_h$ | Pseudo-static coefficient for horizontal earthquake loading |
| $P_i$ | Total reaction normal to the base of the $i^{th}$ slice |
| $Q_i$ | Resultant inter-slice force of the $i^{th}$ slice |
| $S$ | Total shear force available |
| $F$ | Factor of safety |
| $b_i$ | Width of slice |
| $q$ | Surcharge intensity of overburden |
| $h_G$ | Height to centre of gravity from the middle of slice-base |
| $h_Q$ | Height to intersection of resultant inter-slice force from the middle of slice-base |
| $x_{Qi}$ | x coordinate of point $R$ |
| $y_{Qi}$ | y coordinate of point $R$ |

**Figure 2.** Forces acting upon the $i^{th}$ slice

The formulation of equilibrium equations using the Morgenstern and Price method can be found in Zolfaghari et al. [11]. For brevity, only important equations are shown here. By considering the equilibrium of the $i^{th}$ slice, the resultant inter-slice force $Q_i$ can be written as

$$Q_i = \frac{\frac{c' b_i \sec\alpha_i}{F} + \frac{\tan\phi'}{F}(W_i\cos\alpha_i - W_i a_v\cos\alpha_i - W_i a_h\sin\alpha_i + q b_i\cos\alpha_i - u b_i\sec\alpha_i) - W_i\sin\alpha_i + W_i a_v\sin\alpha_i - W_i a_h\cos\alpha_i - q b_i\sin\alpha_i}{\cos(\alpha_i - \theta_i)(1 + \tan(\alpha_i - \theta_i)\frac{\tan\phi'}{F})} \quad (1)$$

In addition, the sum of the overall moments of resultant inter-slice forces about any arbitrary point is equal to zero. As a result, taking moment of inter-slice forces about the origin yields

$$\sum_{i=1}^{n}\left[y_{Qi}(Q_i\cos\theta_i)+x_{Qi}(Q_i\sin\theta_i)\right]=0\,. \tag{2}$$

Similarly, the sum of the vertical and horizontal inter-slice forces must be zero, i.e.,

$$\sum_{i=1}^{n}Q_i\cos\theta=0\,, \tag{3}$$

$$\sum_{i=1}^{n}Q_i\sin\theta=0\,. \tag{4}$$

According to the method of Morgenstern and Price, the ratio between the vertical and horizontal inter-slice forces is assumed to be equal to $\lambda f(x)$, where $\lambda$ is a constant and $f(x)$ is some appropriate function. In most cases, the function $f(x)$ is taken as 1 [11, 13] or sin($cx$) [14, 15], where $c$ is a constant. In this study, $f(x)$ is assumed to be 1. Denoting the horizontal angle of the resultant inter-slice force $Q_i$ as $\theta_i$ gives $\tan\theta_i=\lambda f(x_i)$, where $x_i$ represents the horizontal coordinate $x$ of the center of the $i^{th}$ slice. In Eqs. 2 to 4, there are two unknowns, i.e., the safety factor $F$ and the constant $\lambda$. In this study, Eqs. 2 and 3 will be used to solve for these two unknowns. As aforementioned, the Newton-Raphson method is employed to do this task. The initial value of $\lambda$ for the Newton-Raphson method is assumed to be a fixed empirical value of $0.7\tan\beta$ [15]. Here, the angle $\beta$ is the inclination of the slope surface defined in Figure 1. In addition, the initial value of $F$ is set to unity. These initial guesses have a considerable effect on the convergence rate to the solution.

## 3. Ant colony optimization

### 3.1. Real ants

Ants are social insects and their colonies are highly structured social organizations. As a result, they are capable of accomplishing complex tasks beyond the capabilities of a single ant. The ant colony optimization (ACO) is devised from the foraging behaviour of real ants. Ants are capable of finding the shortest path between a food source and its nest without any visual clues. In fact, ants employ the chemical substance called "pheromone" for indirect communication between them. Ants drop pheromone while walking and they tend to follow trails that have high level of pheromone. This pheromone trail-following mechanism enables them to find the shortest path to the food. Figure 3 illustrates the simple mechanism of finding the shortest path.

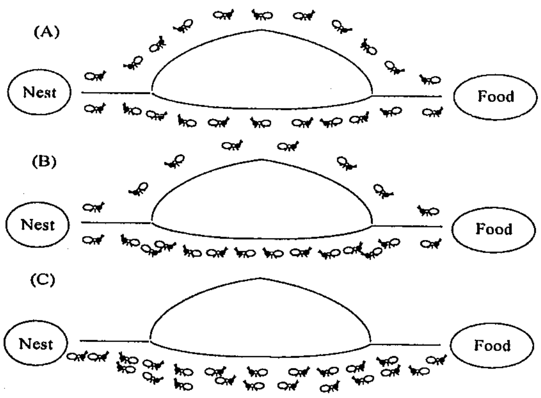


(A) At the beginning, ants select the longer and shorter paths with equal probability.
(B) Pheromone accumulates at a higher rate on the shorter path. More ants select the shorter path.
(C) Finally, all ants virtually select the shorter path

**Figure 3.** How real ants find the shortest path

### 3.2. Ant colony optimization for slope stability analysis

The objective of using ACO in this particular geotechnical problem is to find the critical failure surface, which gives the minimum value of factor of safety. In this study, a slip surface is represented as a piecewise linear line as shown in Figure 4. Define the variable vector **A** to represent slip surfaces in the ACO process as

$$\mathbf{A} = \begin{bmatrix} \hat{x} & \alpha_1 & \Delta\alpha_1 & \Delta\alpha_2 & \cdots & \Delta\alpha_{n-1} \end{bmatrix}^T, \tag{5}$$

where $\hat{x}$ is the initiation point of the slope failure. In addition, $\alpha_1$ is the angle of the slip surface for the 1st slice while $\Delta\alpha_1, \Delta\alpha_2, \ldots,$ and $\Delta\alpha_{n-1}$ are the angle changes from the previous slip lines for the 2nd to $n$th slices (see Figure 4). In this study, $\Delta\alpha_i$ is assumed positive in order to avoid unrealistic slip surfaces. In the proposed ACO algorithm, each ant will select $\hat{x}, \alpha_1, \Delta\alpha_1, \Delta\alpha_2, \ldots,$ and $\Delta\alpha_{n-1}$ from available lists of values and the selection will be interpreted as a possible slip surface. For each variable in $\mathbf{A}$, its available choices are called sub-paths. The overall concept of the proposed ACO algorithm is illustrated in Figure 5.

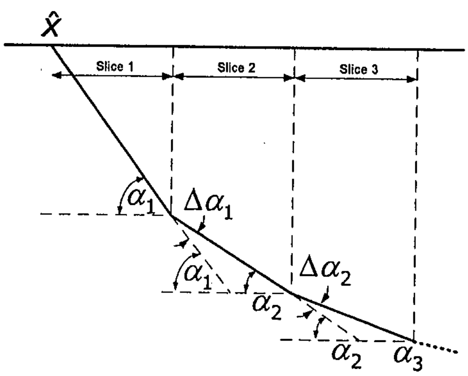


$$\begin{aligned} \alpha_1 &= \alpha_1 \\ \alpha_2 &= \alpha_1 - \Delta\alpha_1 \\ \alpha_3 &= \alpha_2 - \Delta\alpha_2 \\ &\vdots \\ \alpha_n &= \alpha_{n-1} - \Delta\alpha_{n-1} \\ \alpha_1 &> \alpha_2 > \cdots > \alpha_n \end{aligned}$$

**Figure 4.** Representation of a slip surface

According to the foregone discussion, there are $n$+1 distinct variables to be optimized where the $n$ is the number of slices. The ranges of the variables used in this study are shown in Table 1. These ranges are selected in such a way to avoid the local failure of the slope. For each ant, the safety factor $F$ that the ant represents is calculated by solving Eqs. 2 and 3 via the Newton-Raphson method. In ACO, the colony will make a tour from the left side of Figure 5 to the right side repeatedly. In the first tour, all ants will select their paths randomly. From the second tour onward, the ants will probabilistically select their paths that have high levels of pheromone. This can be implemented by setting the probability of a sub-path being selected by an ant in tour $t$ as

$$p(A_i^a,t)=\frac{\tau(A_i^a,t)}{\sum_{k=1}^{S_i}\tau(A_i^k,t)}. \tag{6}$$

Here, $p(A_i^a,t)$ denotes the aforementioned probability where $A_i^a$ represents the $a^{th}$ sub-path for variable $i$. In addition, $S_i$ denotes the total number of available sub-paths for variable $i$. Finally, $\tau(A_i^a,t)$ denotes the amount of pheromone of sub-path $A_i^a$ in tour $t$.

While walking, the ants will lay pheromone on their paths. The amount of pheromone that each ant will lay depends on the quality of the ant's path. In this study, the quality function $\hat{Q}(\mathbf{A})$ is defined as

$$\hat{Q}(\mathbf{A})=\frac{1}{1+F(\mathbf{A})}. \tag{7}$$

It can be seen that the paths that have smaller factors of safety will result in larger values of $\hat{Q}(\mathbf{A})$. Subsequently, these paths will receive higher amounts of pheromone. The pheromone-updating scheme can be written as

$$\begin{aligned}
&\tau(A_i^k,t)=0 && t=1,\\
&\tau(A_i^k,t+1)=\Delta\bar{\tau}(A_i^k,t) && t=1,\\
&\tau(A_i^k,t+1)=(1-\rho)\tau(A_i^k,t)+\rho\Delta\bar{\tau}(A_i^k,t) && t\geq 2.
\end{aligned} \tag{8}$$

Here, $\Delta\tau(A_i^k,t)$ denotes the amount of pheromone laid on sub-path $A_i^k$ in tour $t$. The function $\Delta\tau(A_i^k,t)$ is set proportional to the quality function $\hat{Q}(\mathbf{A})$. The scalar $\rho$ denotes the evaporation factor. This factor is used to control the evaporation rate. It can be seen from Eq. 8 that the evaporation is implemented by the term $(1-\rho)\tau(A_i^k,t)$ while the pheromone laying is implemented by the term $\rho\Delta\bar{\tau}(A_i^k,t)$ .

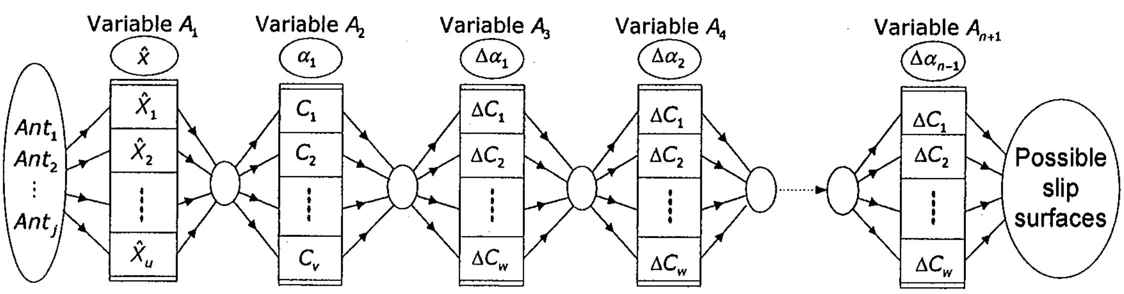


*$j,u,v,w$ are values defined according to the problem definition*

**Figure 5.** Ant touring for finding the critical failure surface

**Table 1.** Parameter ranges for slip surfaces

| Parameter | Range |
|---|---|
| $\hat{x}$ | Problem dependent |
| $\alpha_1$ | Around Rankine's failure angle |
| $\Delta\alpha_1, \Delta\alpha_2, \ldots,$ and $\Delta\alpha_{n-1}$ | 0° to 5° (depending upon the slope geometry) |

## 4. Examples

In order to examine the validity and efficiency of the proposed search algorithm, it is used to solve complex soil slopes under both homogeneous and non-homogeneous conditions. To this end, a wide variety of problems is tested and two examples are shown with comparison here for brevity. Additionally, the effect of earthquake forces is also analyzed.

*Example 1.*

This example is abstracted from Fredlund and Krahn [14] and Figure 6 shows the geometry of the slope used. Recently, Solati and Habibagahi [16] successfully analyzed this slope using a genetic algorithm. The soil is assumed homogeneous with $\phi = 20^\circ$, $c = 29$ kPa and $\gamma = 19.4$ kN/m$^3$. In this study, the slice width is taken as 0.25 m and 300 slices are used. For the ACO algorithm, the values of $\hat{x}$ from 0 to 20 m with the accuracy of 0.25 m are used. For $\alpha_1$ and $\Delta\alpha_i$, the ranges from 0° to 55° and from 0° to 2.5° are, respectively used. For both ranges, the same interval size of 0.01° is employed. A pseudo-static coefficient for horizontal earthquake loading $a_h$ of 0.1 is used for the analysis. The number of ants and the number of tours used in this problem are 300 and 100, respectively. The evaporation rate of pheromone $\rho$ is set as 0.3. The results obtained from this study are presented and compared with the existing results from the literature in Table 2. It can be seen from the comparison that the obtained results agree well with the existing results.

**Table 2.** Minimum factors of safety for Example 1

| Source | Limit equilibrium method | Optimization method | $F$ without water table | $F$ with water table |
|---|---|---|---|---|
| Fredlund and Krahn [14] | Ordinary | Best-fit regression | 1.928 | 1.693 |
| | Simplified Bishop | Best-fit regression | 2.080 | 1.834 |
| | Spencer | Best-fit regression | 2.073 | 1.830 |
| | Janbu's simplified | Best-fit regression | 2.041 | 1.827 |
| | Janbu's rigorous | Best-fit regression | 2.008 | 1.776 |
| | Morgenstern and Price | Best-fit regression | 2.076 | 1.833 |
| Solati and Habibagahi [16] | Generalized | GA | 2.079 | 1.840 |
| This study | Morgenstern and Price | ACO | 1.996 | 1.801 |
| This study (with earthquake) | Morgenstern and Price | ACO | 1.799 | 1.432 |

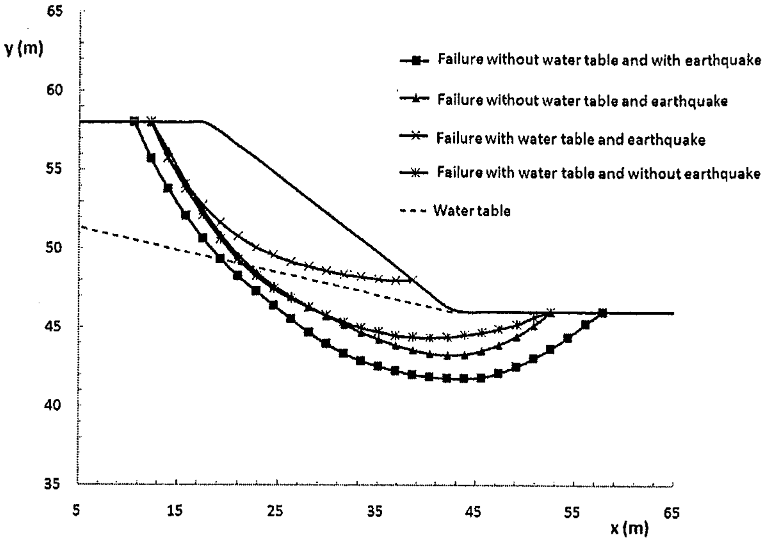


**Figure 6.** Critical failure surfaces for Example 1

*Example 2.*

A multilayer slope consisting of a sand layer( Layer 1) over a clay layer ( Layer 2) with a water table shown in the Figure 7 is analyzed. There is a firm hard layer located underneath the clay layer. The example is taken from Joseph Spigolon [17]. Soil parameters for the sand layer are taken as $c = 0$, $\phi = 25^{\circ}$ and $\gamma = 120$ pcf. For the clay layer, they are taken as $c = 600$ psf, $\phi = 25^{\circ}$ and $\gamma = 92$ pcf. Two loading cases with and without the effect of earthquake loading are considered. The slice width is taken as 1 ft and 150 slices are considered. The values of all ACO parameters as well as the ranges of $\hat{x}$, $\alpha_1$, and $\Delta\alpha_i$ are kept the same as those used in the previous example. The obtained results are presented in Table 3. Similar to the previous example, good agreement can be observed in the comparison with the results from the literature.

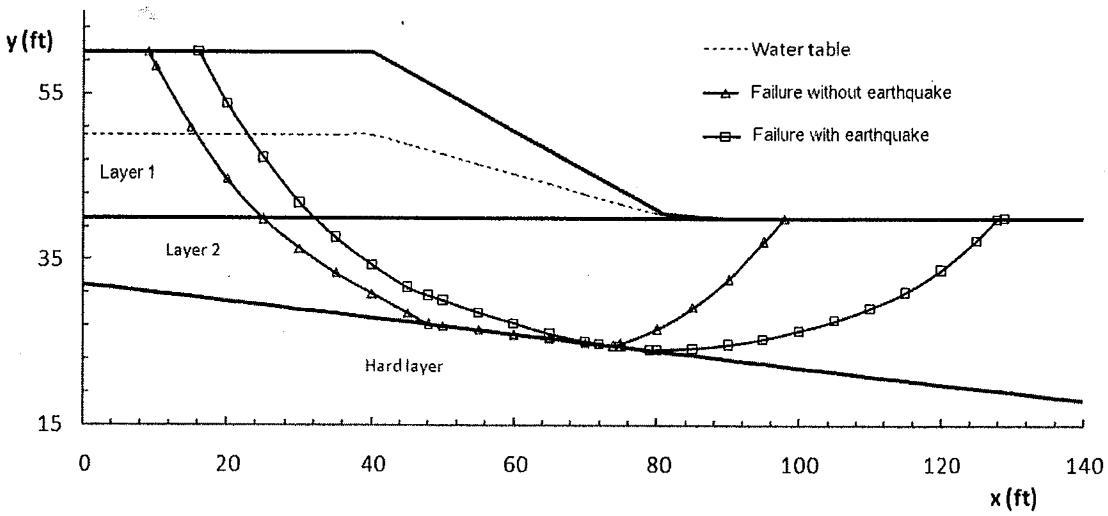


**Figure 7.** Critical failure surfaces for Example 2

**Table 3.** Minimum factors of safety for Example 2

| Source | Limit equilibrium method | Optimization method | *F* |
|---|---|---|---|
| Joseph Spigolon [17] | Method of wedge | – | 1.27 |

| | | | |
|---|---|---|---|
| This study | Morgenstern and Price | ACO | 1.096 |
| This study (with earthquake) | Morgenstern and Price | ACO | 0.841 |

## 5. Conclusion

Based on the mechanism of foraging behaviour of ants, the ACO metaheuristic algorithm is implemented for slope stability analysis problems. The main concept of the proposed method is to use ACO to find the slip surface that has the lower factor of safety. The numerical examples used in the paper show that the proposed method can be successfully used for difficult problems governed by some special geotechnical features. The results obtained from this study are compared with some existing results in the literature and are found to be satisfactory. It can be said that the proposed method is an efficient method for slope stability analysis.

**References:**


[1] Morgenstern, N. R. and Price, V. E., The analysis of the stability of general slip surfaces, Geotechnique, 1965, 79-93.

[2] Spencer, E., A method of analysis for stability of embankments using parallel inter-slice forces, Geotechnique, 1967, 11-26.

[3] Bishop, A. W., The use of the slip circle in the stability analysis of earth slopes, Geotechnique, 1955, 7-17.

[4] Janbu, N., Slope stability computations, Hirschfield and S. Poulos, New York, 1973.

[5] Baker, R., Determination of the critical slip surface in slope stability computations, 1980, 333-359.

[6] Malkawi, H., et al., Global search method for locating general slip surface using Monte Carlo technique., Journal of Geotechnical and Geoenvironmental Engineering, 2001, 688-698.

[7] Greco, V. R., Efficient Monte Carlo technique for locating critical slip surface, Journal of Geotechnical Engineering, ASCE, 1996, 517-525.

[8] Goh, T. C., Search for critical slip circle using genetic algorithms, Civil Engineering and Environmental Systems, 2000, 181-211.

[9] McCombie, P. and Wilkinson, P., The use of the simple genetic algorithm in finding the critical factor of safety in slope stability analysis, Computers and Geotechnics, 2002, 699-714.

[10] Das, S. K., Slope stability analysis using genetic algorithm, Electron. J. Geotech. Engrg., 2005,

[11] Zolfaghari, A. R., et al., Simple genetic algorithm search for critical non-circular failure surface in slope stability analysis, Computers and Geotechnics, 2005, 139-152.

[12] Jianping, S., et al., Search for critical slip surface in slope stability analysis by by spline-based GA method. , Journal of Geotechnical and Geoenvironmental Engineering, 2008, 252-256.

[13] Yamagami, T. and Ueta, Y., Search for noncircular slip surfaces by the Morgenstern-Price method, 6th International Conference of Numerical Methods in Geomechanics, 1988, 1219-1223.

[14] Fredlund, D. G. and Krahn, J., Comparison of slope stability methods of analysis, Canadian Geotechnical Journal, 1977, 429-439.

[15] Zhu, D. Y., et al., A new procedure for computing the factor of safety using the Morgenstern-Price method, Canadian Geotechnical Journal, 2001, 882-888.

[16] Solati, S. and Habibagahi, G., A genetic approach for determining the generalized inter-slice forces and the critical non-circular slip surface, Iranian Journal of Science & Technology, 2005,

[17] Spigolon, S. J., The McGraw-Hill civil engineering PE exam depth guide : geotechnical engineering / S. Joseph Spigolon., McGraw Hill, New York, 2001.

# GEOTECH GROUP

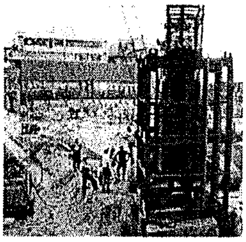

## GEOTECH LIMITED

**THE PREMIER SOIL INVESTIGATION COMPANY**

* ON SHORE & OFF SHORE SOIL INVESTIGATIONS & DEEP DRILING

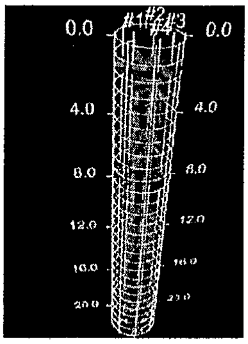


* CONE PENETRATION TESTS
* PLATE LOAD TESTS
* GROUND WATER INVESTIGATIONS

## GEOTECH TESTING SERVICES (PVT) LTD

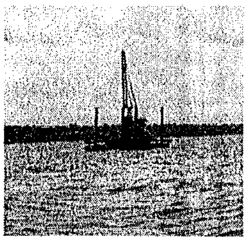

PIONEERS IN SRI LANKA FOR ELECTRONIC PILE TESTS

* PILE INTEGRITY TESTS & PILE DYNAMIC ANALYSIS
* SONIC LOGGING TESTS
* ROCK ANCHOR TESTS

13/1, PEPILIYANA MAWATHA, KOHUWALA, SRI LANKA.
TEL: 281 3805, 071 473 5745 TEL\FAX: 2823881
WEBSITE: www.geotechlanka.com
E-MAIL: geotech@eureka.lk

## GROUP ENGINEERING LABORATORIES LTD

LABORATORY TESTING FOR CONSTRUCTION INDUSTRY AND FIELD LABORATORY, & WATER QUALITY

465/1 SUNETHRADEVI ROAD, PEPILIYANA, NUGEGODA.
TEL: 2769828, 0714735745

# Suitability of Quarry Dust in Geotechnical Applications to Improve Engineering Properties

N. H. Priyankara, R. M. S. D. Wijesooriya, S. N. Jayasinghe, W. R. M. B. E. Wickramasinghe and S. T. A. J. Yapa

**Abstract:** Quarry dust is a by-product of rubble crusher units and a commonly available material due to the vast usage of crusher metal in construction industry. This product can be used to improve engineering properties of high plasticity silty (MH) soils, in order to develop a cost effective method for highway sub grade construction. As such, research reported in this paper illustrates the effect of usage of quarry dust as an admixture to improve the engineering properties of high plasticity silty soils with combination of cement. High plasticity silty soils which were rejected by the one of the main road construction projects in Sri Lanka were selected as the test samples. These high plasticity silty soils were mixed in the laboratory with different percentages of quarry dust and 2 % of cement on the weight and left to harden for a period of seven days. Further, shear strength behavior of soil-quarry dust mixes were presented in this paper. The results of the subsequent tests revealed that even mixing with only quarry dust caused appreciable improvement in engineering characteristics of poor quality soils. It was found that this improvement can be significantly enhanced with the addition of 2 % of cement. Therefore, problems associated in the construction of highways over clayey sub grade can be reduced significantly by mixing with quarry dust and cement.

**Keywords:** High Plasticity Silty Soil, Quarry Dust, CBR Value

## 1. Introduction

With the developments taking place in the country, there is a scarcity of lands with good sub soil conditions. Therefore, civil engineers are compelled to build new structures and infrastructure facilities in areas where existing ground conditions are not very favorable. In Sri Lanka, numbers of new projects are proposed at locations where there are soft clays/ high plasticity silty soils with substantial thickness.

Construction on soft clay/ high plasticity silty soils leads to stability problems during the construction and long term settlements during the service due to its very low shear strength and very high compressibility. Although the heavy loads from the super structure of multistory buildings can be transferred to an underlying hard stratum through piled foundations, it is not an economical form of foundations when the roads and service lines are to be constructed. In such situations the use of shallow foundations after the improvement of the soft soil/ high plasticity silty soil layer will be a more economical option.

Different methods are available for the improvement of compressibility and shear strength characteristics of soft soil and high plasticity silty soils. These methods can be classified primarily as densification processes and solidification processes. In addition, replacement method is also very commonly used in the developing countries.

Preloading and dynamic compaction are some of the most widely used densification processes. In the past, preloading method was the most commonly used method to improve soft soil in developing countries. The main criticism against the preloading is the rather long time period required for the process. With the development taking place in the country, necessity of quick, economical and effective methods to improve soft/ high plasticity silty soil are rising up. Therefore, it is a responsibility of geotechnical engineers and scientists to find appropriate methods to improve soft/ high plasticity silty soil.

*N. H. Priyankara, B.Sc. Eng. (Moratuwa), M.Eng. (AIT), PhD(Tohoku), Senior Lecturer, Department of Civil and Environmental Engineering, University of Ruhuna, R. M. S. D. Wijesooriya, B.Sc. Eng. (Ruhuna), Former student, Department of Civil and Environmental Engineering, University of Ruhuna, S. N. Jayasinghe, B.Sc. Eng. (Ruhuna), Former student, Department of Civil and Environmental Engineering, University of Ruhuna, W. R. M. B. E. Wickramasinghe, B.Sc. Eng. (Ruhuna), Former student, Department of Civil and Environmental Engineering, University of Ruhuna, and S. T. A. J. Yapa, B.Sc. Eng. (Ruhuna), Former student, Department of Civil and Environmental Engineering, University of Ruhuna.*

As a result many researches have paid their attention to use waste/by-products as construction materials to improve soft soil, especially in highway construction. In this research study, applicability of quarry dust, which is a by-product of metal crusher units, to improve sub grade materials in pavement construction in highways was studied.

Quarries and aggregate crushers are basic requisites for construction industry. Rubble crushing is processed for use as construction aggregate consisting of blasting, primary and secondary crushing, screening and stockpiling operation. Quarry dust is a by-product of rubble crushing operation and is one of the newly found materials used for the ground improvement in highway construction, building industry etc, especially in developing countries. By a rough estimation about million tons of quarry dust is been generated in each year as a by-product. Gradation of this material does not satisfy the specification requirements for concrete works. This is mainly due to fine state of quarry dust resulting in large specific surface. In this background any attempt to utilize this by-product in highway construction is useful.

A review of literature indicates that, in India, quarry dust has been extensively utilized in geotechnical applications such as embankments, highway sub grades etc (Soosan et al., 2005). Further, many researches (Gidley and Sack, 1984; Kamon et al., 1989; Rao and Reddy, 1989) have utilized other industrial wastes such as fly ash, marble dust to stabilize the soft soils. There are limited information available about the utilization of industrial waste combined with cement or lime to improve the engineering characteristics of poor quality soils. The research reported in this paper, an attempt was made to improve the engineering properties of high plasticity silty soils, which were rejected by the consultants of one of the major highway construction sites in Sri Lanka, mixing with different proportions of quarry dust and 2 % of cement.

Results obtain in this study will help to solve the problems associated with highway construction over the high plasticity silty soils to a considerable extent and which may contribute towards the economy in construction of highways.

## 2. Materials and Methodology

### 2.1 Materials

Quarry dust samples were collected from three different rubble crusher units (Location 1, 2 and 3) near to the faculty premises. Particle size distribution of quarry dust samples from different locations are presented in Figure 1. It can be seen from the figure that quarry dust mainly consists of sand size particles; fine sand ranging from 23.3 to 26.9 %; medium sand ranging from 31.0 to 41.4 %; coarse sand ranging from 15.4 to 23.6 %. Even though the samples are collected from different locations and different quarries, variation in particle size distribution is marginal. Since the lowest gravel percentage is obtained from the rubble crusher unit at Location 2, which was selected for collecting quarry dust materials for this research study. Physical properties of the selected quarry dust sample are illustrated in Table 1.

Poor quality soil samples which were rejected by the consultants of one of the main road construction projects in Sri Lanka, were selected for this research study. Particle size distribution and physical properties of the selected soil sample are depicted in Figure 1 and Table 1 respectively along with the data of quarry dust. The soils possess relatively high liquid limit and relatively high plasticity index, which does not satisfy the Road Development Authority (RDA) highway pavement construction specifications. Further, particle size distribution of soil sample possesses a large percentage of silt and clay. According to the Unified Soil Classification System (USCS) this soil can be classified as High Plasticity Silt (MH).

### 2.2 Experimental Investigation on Soil-Quarry dust mixtures

Different percentages of quarry dust varying between 0 to 100 % in steps of 20 % on dry weight were mixed with high plasticity silty soils using a mechanical mixer. Sample prepared by mixing four parts of soil (80 %) with one part of quarry dust (20 %) on dry weight is designated as S-20. In similar lines, in samples S-40, S-60 and S-80, quarry dust content was 40, 60 and 80 % respectively on total dry weight of the mixture. Unimproved soil is represented as S-0 where as quarry dust alone is designated as S-100.

**Table 1 - Physical properties of quarry dust and high plasticity silty soil**

| Properties | Quarry dust | Soil |
|---|---|---|
| Soil type according to USCS | SM | MH |
| Specific gravity | 2.64 | 2.49 |
| Maximum dry density( kg/m³) | 2101.93 | 1243.90 |
| Optimum moisture content (%) | 10.00 | 35.00 |
| Unsoaked CBR value (%) | 61.18 | 11.67 |
| 4 day soaked CBR value (%) | 48.00 | 2.90 |
| Liquid Limit (LL) (%) | 27.00 | 73.50 |
| Plastic Limit (PL) (%) | Non-plastic | 38.20 |
| Plasticity Index (PI) (%) | 0.00 | 35.30 |

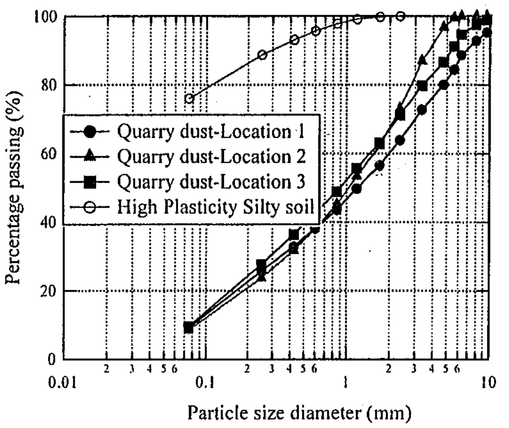


**Figure 1 - Particle size distribution of quarry dust and high plasticity silty soil**

Particle size distributions of soil-quarry dust combinations are presented in Figure 2. It can be seen that percentage of sand content gradually increases with the addition of quarry dust. Conversely, it can be noted that percentage of silt and clay content decreases with the increase of percentage of quarry dust. The physical properties of the soil-quarry dust combinations are illustrated in Table 2.

It is well known that liquid limit of a particular soil is determined using Atterberg limit apparatus which is commonly named as Casagrande's method. However, difficulties are encountered in cutting a groove in order to determine the liquid limit of soil-quarry dust mixtures when the percentage of quarry dust increases (Sheerwood and Ryley, 1970; Soosan et al., 2005). In order to overcome these problems, Sheerwood and Ryley (1970) proposed to use Cone Penetrometer to determine liquid limit. As such, in this research study, liquid limit of soil-quarry dust mixture were determined using Cone Penetrometer method according to BS 1377-Part 2.

Compaction tests were conducted for all soil-quarry dust mixtures using the Standard Proctor Compaction test. The CBR (California Bearing Ratio) tests under both unsoaked and 4 day soaked condition were conducted based on the results of Standard Proctor Compaction test for all soil-quarry dust mixtures. Further, direct shear test on samples compacted at optimum moisture content were conducted in order to investigate the shear strength characteristics of soil-quarry dust mixtures (Wijesooriya et al., 2008).

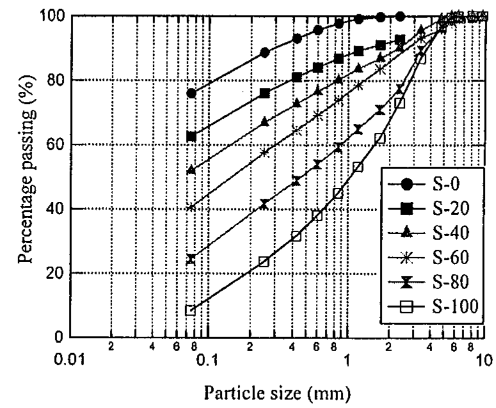


**Figure 2 - Particle size distribution of soil-quarry dust mixtures**

### 2.3 Experimental Investigation on Soil-Quarry Dust-Cement Mixtures

In order to further improve the engineering characteristics of poor quality soil, cement was added to the soil-quarry dust mixture. Kulathilaka et al. (2001) has been found that, engineering properties of peat can be sufficiently improved with mixing 5 % of cement. Based on this fact, 5 % of cement on dry weight was mixed with S-40 sample which was taken as the trial sample.

Three soil-quarry dust-cement samples were prepared, in order to find the CBR at unsoaked, 4 day soaked and 7 day soaked conditions. Results of this pilot test are presented in Table 3. It is a well known factor that concrete achieves its full unconfined compressive

Table 2 - Physical properties of soil-quarry dust mixtures

| | Liquid Limit (%) | Plastic Limit (%) | Maximum dry density (kg/m$^3$) | Optimum moisture content (%) | 4 day soaked CBR value (%) | Unsoaked CBR value (%) |
|---|---|---|---|---|---|---|
| S-0 | 73.50 | 38.2 | 1243.90 | 35.00 | 2.90 | 11.67 |
| S-20 | 67.00 | Non-plastic | 1413.86 | 27.50 | 3.00 | 11.25 |
| S-40 | 54.50 | Non-plastic | 1529.05 | 22.50 | 3.67 | 16.10 |
| S-60 | 43.25 | Non-plastic | 1766.56 | 15.50 | 5.57 | 23.20 |
| S-80 | 32.25 | Non-plastic | 1938.83 | 12.60 | 13.80 | 33.35 |
| S-100 | 27.00 | Non-plastic | 2101.93 | 10.00 | 48.00 | 61.18 |

strength within 28 days and 70 % of the unconfined compressive strength within 7 days. Further, due to the long testing period of durability test (28 days), many highway agencies currently use 7 day unconfined compressive strength values for cement treated soils (Zhang and Tao, 2008). Therefore, in addition to the conventional 4 day soaked CBR value, 7 day soaked CBR value was determined for soil-quarry dust-cement mixture as shown in Table 3.

It can be seen that CBR values have been increased significantly with the addition of 5 % of cement. A noticeable increase in 7 day soaked CBR value can be observed over the 4 day soaked CBR value due to the hardening effect of the cement. Therefore, it was decided to check only the 7 day soaked CBR value instead of conventional 4 day soaked CBR value for the cement treated soil-quarry dust mixtures.

Due to the significant improvement of CBR value with mixing 5 % of cement on soil-quarry dust mixture, it was decided to reduce the cement percentage, in order to reduce the cost. As show in the Table 3, there was no improvement with the addition of 0.5 % of cement. Therefore, 2 % of cement was added to soil-quarry dust mixture in order to achieve a substantial improvement in CBR value. Zhang and Tao (2008) also indicated that in order to achieve a substantial improvement in unconfined compressive strength in cement treated soil, cement percentage should be greater than 2.5 %. Therefore, the selected cement percentage in this research is almost comparable with the literature.

## 3. Results and Discussion

### 3.1 Liquid Limit

Variation of liquid limit with the addition of quarry dust is presented in Figure 3. It can be seen that liquid limit of soil-quarry dust mixtures linearly decreases with the increase of quarry dust percentage. About 45 % reduction in liquid limit with respect to unimproved soil can be observed with the addition of 60 % of quarry dust. This indicates that cohesive nature caused by the absorbed water surrounding the clay particles reduces with the addition of quarry dust. Another notable feature is that all combinations of soil-quarry dust mixtures show non-plastic behaviour, i.e. plasticity index of all combinations of soil-quarry dust mixture equal to zero.

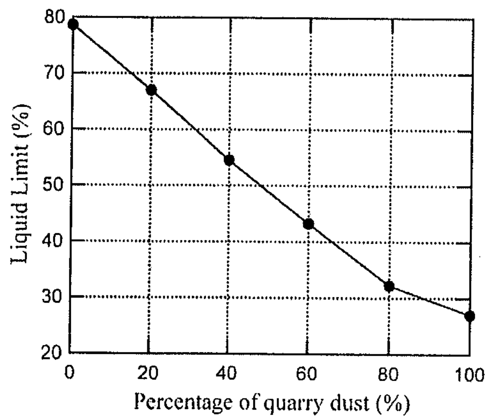


**Figure 3 - Variation of liquid limit of soils with the addition of quarry dust**

### 3.2 Shear Strength Characteristics

Figure 4 illustrates the variation of internal friction angle and cohesion of soil-quarry dust mixtures with respect to percentage of quarry dust. It can be noted that addition of quarry dust to soil reduces the cohesion whereas increases the friction angle. A significant variation in shear strength characteristics can be observed when the quarry dust percentage varies from 20 to 60 %. Conversely, no significant variation can be achieved when the quarry dust percentage is greater than 60 %. These results clearly indicated that addition of quarry dust is more effective when quarry dust

**Table 3 - CBR values of soil-quarry dust-cement mixtures**

| Quarry dust percentage (%) | Cement percentage (%) | CBR value (%) | | |
|---|---|---|---|---|
| | | Unsoaked | 4 day soaked | 7 day soaked |
| 40 | 5.0 | 24.00 | 76.70 | 173.20 |
| 40 | 0.5 | 5.68 | - | 4.76 |
| 40 | 2.0 | 13.22 | - | 73.57 |

percentage is 20-60 % with respect to shear strength characteristics.

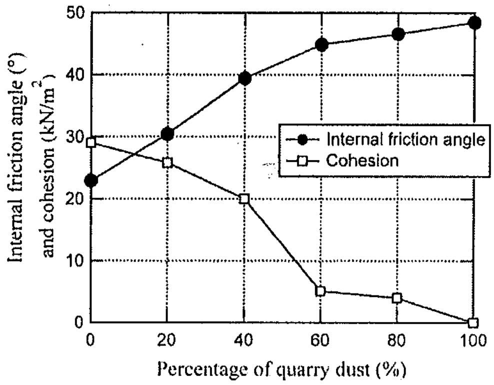


**Figure 4 - Variation angle of internal friction and cohesion with the addition of quarry dust**

### 3.3 Compaction Characteristics

Standard Proctor Compaction curves for soil-quarry dust mixtures are presented in Figure 5. It can be seen that unimproved soil gives an almost flat curve. Conversely, quarry dust shows the highest value of maximum dry density and the lowest value of optimum moisture content compared to unimproved soil. This is mainly because of the coarser of solid particles and high specific gravity of quarry dust.

The compaction curve of unimproved soil (S-0) which is relatively flat shows more and more pronounced peak with the addition of quarry dust. The variations of maximum dry density and optimum moisture content over the percentage of quarry dust are presented in Figure 6.

It can be noted that addition of any amount of quarry dust tò soil increases maximum dry density and decreases optimum moisture content considerably. Results indicated that percentage increment in maximum dry density and percentage reduction in optimum moisture content are significant when addition of quarry dust percentage vary from 40 to 60 %. It is a notable feature that maximum dry density can be improved to 1600 kg/m³ which is the RDA requirement for sub grade construction in highways with the addition of 47 % of quarry dust. This is a 23 % increment in maximum dry density and 43 % reduction in optimum moisture content.

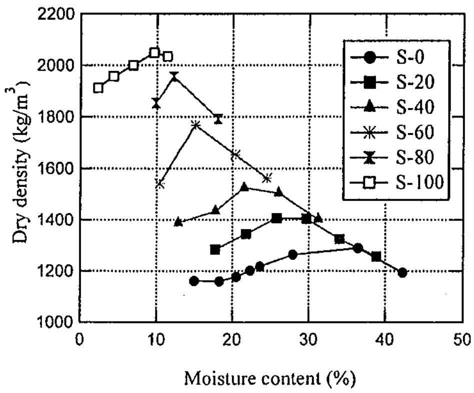


**Figure 5 - Compaction curves for soil-quarry dust mixtures**

### 3.4 California Bearing Ratio (CBR)

The variations of CBR values over different soil-quarry dust combinations under both soaked and unsoaked conditions are presented in Figure 7. It can be seen that, there is no improvement in unsoaked CBR value with the addition of 20 % of quarry dust. A noticeable increase in unsoaked CBR value can be observed when the quarry dust percentage is greater than 20 %. It is clear that, there is no improvement in 4 day soaked CBR value until the addition of 40 % of quarry dust. But even after the addition of 60 % quarry dust not much of an improvement is achieved with respect to 4 day soaked CBR value. Considerable improvement in soaked CBR value can be observed with the addition of 80 % of quarry dust. Therefore, in order to achieve a considerable improvement in CBR value, 60-80 % quarry dust content can be taken as the optimum range. Even these values are less than the recommended CBR value (15 %) for sub grade construction in highways according to RDA specification. This indicates that addition of quarry dust alone is not that effective.

In order to further improve the CBR values, cement was added to soil-quarry dust mixtures. Figure 8 indicates the CBR values both under unsoaked and soaked condition with the addition of 2 % of cement to all combinations of soil-quarry dust mixtures. It can be seen that unsoaked and 7 day soaked CBR values significantly increased with the addition of 2 % of cement.

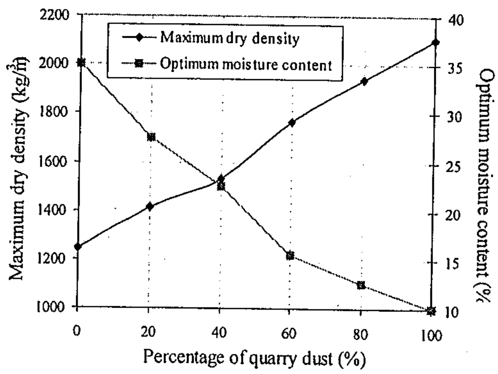


**Figure 6 - Variation of maximum dry density and optimum moisture content of soil-quarry dust mixture over percentage of quarry dust**

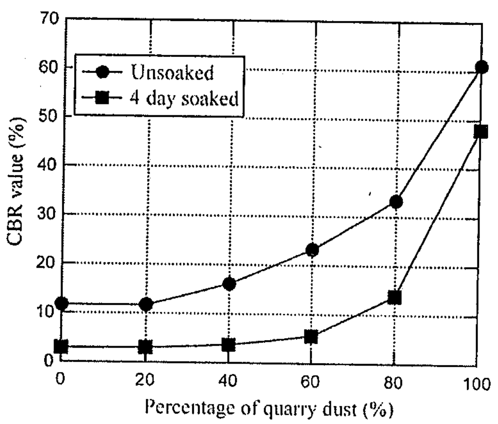


**Figure 7 - Variation of CBR value for different soil-quarry dust mixtures**

The effect of mixing cement with soil-quarry dust mixture on soaked CBR values are illustrated in Figure 9. A noticeable improvement in CBR values can be observed when 2 % of cement mixing with 20-60 % of soil-quarry dust combinations. No significant improvement in CBR values is observed, when the quarry dust content is between 60-80 %. Therefore, 20-60 % of quarry dust content with 2 % cement can be taken as the optimum range, in order to achieve a substantial improvement in engineering properties of high plasticity silty soil.

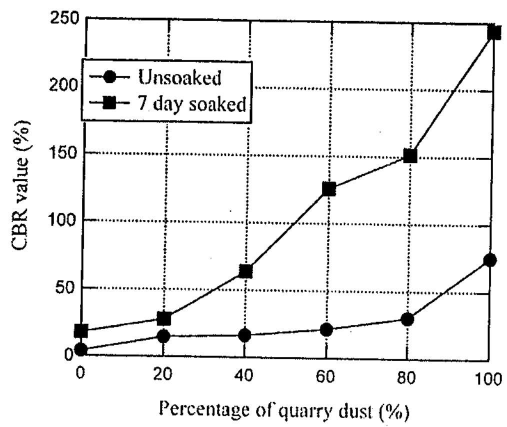


**Figure 8 - Variation of CBR value for different soil-quarry dust mixtures with the addition of 2 % of cement**

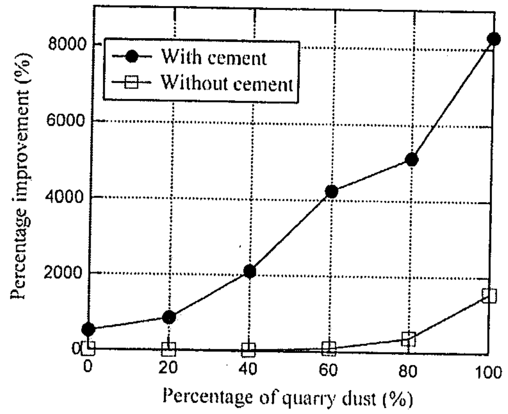


**Figure 9 - Comparison of improvements achieved in CBR values with the addition of cement**

## 4. Conclusions

Improvement of high plasticity silty soils mixing with industrial waste like quarry dust is one of the major challenges faced by Sri Lankan civil engineers. Quarry dust, a by-product of rubble crusher units, consists of mainly sand size particles with high specific gravity and high dry density.

The improvement by mixing with different percentage of quarry dust and 2 % of cement were tried under laboratory conditions and improvements achieved in engineering properties were evaluated. Engineering properties of high plasticity silty soils were improved substantially by the addition of quarry dust. Improvements are manifested in the form of reduction of liquid limit, reduction of plasticity index, increase of internal friction angle and reduction of cohesion.

Addition of quarry dust into high plasticity silty soil is seemed to cause significant improvement in maximum dry density and reduction in optimum moisture content. It was found that highway sub grade construction requirements stated by RDA specification can be achieved with respect to maximum dry density with the addition of 47% of quarry dust into high plasticity silty soil.

The research presented in this paper found that CBR values steadily increased with increase in percentage of quarry dust. Considerable improvement in 4 day soaked CBR value was obtained with the addition of 80 % of quarry dust. Even this value is less than the recommended soaked CBR value (15 %) for highway construction. Further, usage of 80 % of quarry dust cannot be recommended based on the cost factor. Therefore, it was concluded that addition of quarry dust alone to improve the engineering properties of high plasticity silty soil is not much effective.

In order to further improve the CBR values, 2 % of cement was recommended to mixing with soil-quarry dust mixture. It was revealed that 20-60 % quarry dust content with 2 % cement can be taken as the optimum range, in order to achieve a substantial improvement in engineering properties of high plasticity silty soil. Hence it can be concluded that use of quarry dust for geotechnical applications is economically beneficial and environmental friendly.

## References


1. Gidley, J. S., & Sack, W. S., "Environmental Aspects of Waste Utilization in Construction", *J. Environmental Engineering Division*, ASCE, Vol. 110, No. 6, 1984.

2. Kamon, M., Nontananandh, S.,& Katsumi, T., "Effective Utilization of Stainless Steel Slag for Soil Stabilization", *Proc. 24th Japan National Congress on Soil Mechanics and Foundation Engineering*, pp. 1947-1948, 1989.

3. Kulathilaka, S.A.S., Munasinghe, W.G.S. & Priyankara N.H., "Improvement of Engineering Properties of Peat by Cement and Lime Mixing", *Proc. Engineering Research Unit- University of Moratuwa*, 2001.

4. Rao Babu, D., & Reddy Srinivas, B., "Stabilization of Red Soil with Fly Ash", *Proc. Indian Geotechnical Conference*, Vol. 1, pp. 303-306, 1989.

5. Sheerwood, P.T., & Ryley, M.D., "An Investigation of a Cone Penetrometer Method for the Determination of Liquid Limit", *Geotechnique*, Vol. 20, pp. 203-208, 1970.

6. Soosan, T. G., Sridharan, A., Jose, B. T. & Abraham, B. M., "Utilization of Quarry Dust to Improve the Geotechnical Properties of Soils in Highway Construction", *Geotechnical Testing Journal*, Vol. 28, No. 4, pp. 391-400, 2005.

7. Wijesooriya, R. M. S. D., Jayasinghe, S. N., Wickramasinghe, W. R. M. B. E & Yapa, S. T. A. J., "Utilization of quarry dust to improve engineering properties of soils in highway construction", *A Thesis submitted in partial fulfillment of the requirements of B.Sc (Eng) Degree of University of Ruhuna*, 2008.

8. Zhang, Z, & Tao, M., "Durability of Cement Stabilized Low Plasticity Soils", *J. Geotechnical and Geoenvironmetal Engineering*, Vol. 134, No. 2, pp. 203-213, 2008.

*With Best Compliments from*

# LEKAMAGE ASSOCIATES (PVT) LTD

**ENGINEERS & ARCHITECTS**

■ We represent **TENSAR INTERNATIONAL**

World leaders in geogrids

presenting the latest innovation

**TriAx**

**TRIAXIAL GEOGRID**

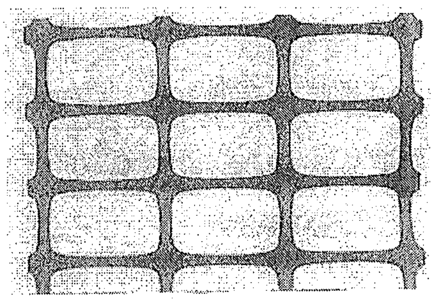

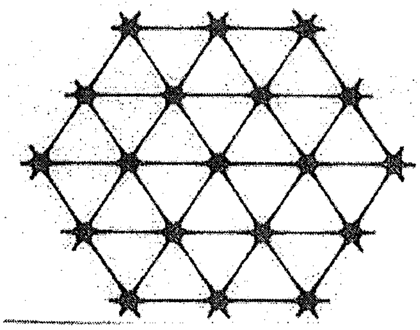

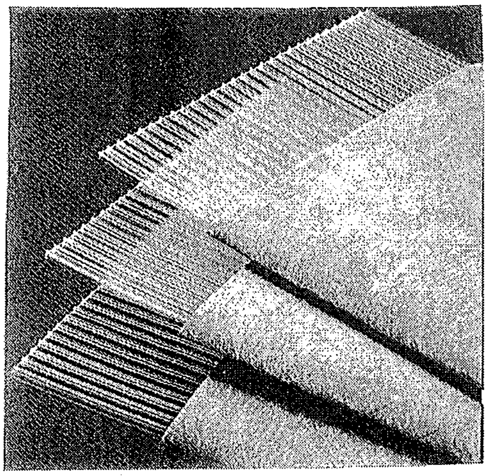

■ We represent **CAPITAL ENVOY (M) SDN BHD**

producing **CeTeau** Wick Drains

PREFAB VERTICAL DRAINS (PVD)

**APPLICATIONS**

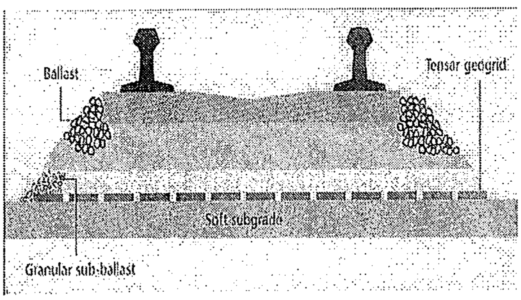


RAILWAY WORKS

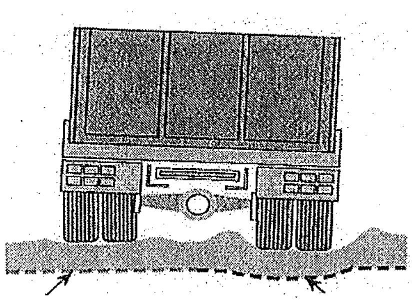

ROADS

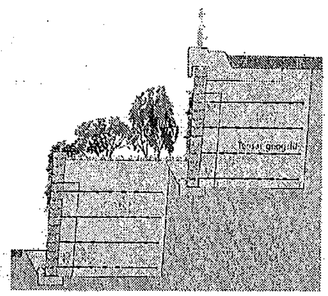

SLOP STABILIZATION

**INQUIRIES**

Address : 33, Vijithapura, Thalawathugoda Road, Pita Kotte
Tel : +94 - 112 868806
Fax : +94 - 112 868805
Mobile : +94 - 777 687243 / 718 444161
E-mail : lrlp6@sltnet.lk / lekamage@sltnet.lk

# DESIGN OF SURFACE AND SUBSURFACE DRAINAGE SYSTEM FOR JOHNSTON ESTATE RESETTLEMENT SITE, NUWARAELIYA USING GIS TECHNIQUE

H.R.Maduranga, B.M.R.K.Balasooriya, National Building Research Organization

**Abstract**

Johnston Estate is one of the places where a proper drainage system is required in order to ensure the safety of residents. Therefore, introduction of a design for proper drainage system for Johnston Estate is the scope of this project. Geographic Information Systems (GIS) for spatially distributed hydrologic and hydraulic modeling is used to achieve the above task. This paper describes the methodology adopted in that site.

**Keywords** - Geographic information system (GIS), Triangular Irregular Networks (TIN), Digital Elevation Model (DEM), Surface Erosion, Geology, Hydrology.

## 1. Introduction

The major disasters occurred in the Central Province of Sri Lanka is due to collapsing of unstable slopes along the slopping ground environment with high rainfall intensity. Natural processes and man-made activities originated along slopping ground are the two major causes of failing slopes in the hill country. In many cases though it seems to be a natural slope failure, man-made activities have become the source of the slope failures.

Among such activities improper drainage systems have become the dominant cause for the slope failures. Surface erosion and rising of ground water table in rainy season occur with improper drainage systems. There are large numbers of places in the hill country where absence of proper drainage systems can lead to failure and ultimately cause lot of damages to the occupants. Johnston Estate is one of the places where a proper drainage system is required in order to ensure the safety of residents. Therefore, introducing a proper drainage system for Johnston Estate is the scope of this project.

## 2. Objective

The main objective of a proper surface drainage system is to collect surface water resulting from heavy rainfall and/or spring and safely discharge it to the nearest natural drainage as quickly as possible.

## 3. Developing geographic information systems (GIS) for "Johnston Estate"

Geographic information system (GIS) was applied for planning of proper drainage system to the Johnston Estate because it can describe the stream pattern, stream direction, amount of the surface water accumulation etc...

Initially the data points were obtained from the surveying details at Johnston Estate (see Fig 01) for preparation of continuous surface model.

The surface model describes the attributes that have the values of every point on the earth. Therefore, it plays a big role in this analysis to understand, describe, or predict scenarios.

For developing the surface, Triangular Irregular Networks (TIN) layers were used. It is typically used for high-precision modeling of smaller areas like Johnston Estate. In engineering applications, TINS are very useful because they allow calculations of planimetric area, surface area and volume.

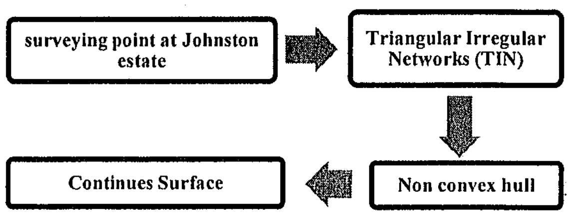


The Digital Elevation Model (DEM) developed using the TIN, is required for the hydrology analysis at this site.

## 4. Digital Elevation Models (DEM) for Johnston Estate

Digital Elevation Models is a raster representation of a continuous surface, usually referencing the surface of the earth. The surface raster is construct using the above TIN with TinRaster_3d function in ArcGIS.

As per the scale and extent of Johnston Estate the cells size of 5m x 5m was selected for developing rasters. The rasters are rectangular arrays of cells (or pixels), each of which stores a value for the part of the surface it covers. A given cell contains a single value, so the amount of detail that can be represented for the surface is limited to the size of the raster cells. Rasters map of Johnston Estate is shown in Fig 03.

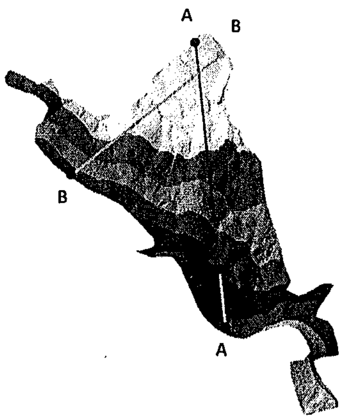


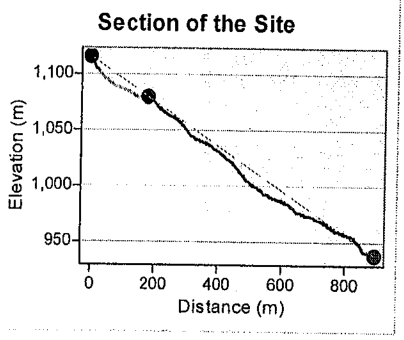


Section A-A

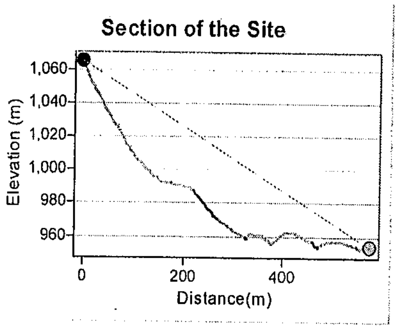


Section B-B

**Fig01:** Surface profiles at the Johnston estate

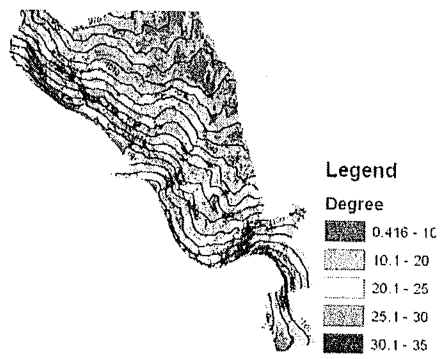


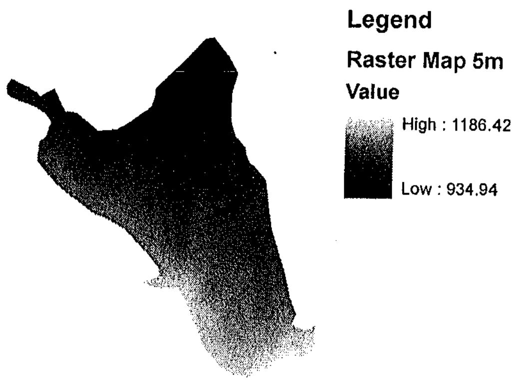


**Fig03:** Rasters map of Johnston Estate

## 5. Geology

About 90% of the country's basement is underlain by late proterozoic high grade metamorphic rock and the rest is made up of Mesozoic (Jurassic), Tertiary (Miocene) and quaternary sedimentary formation. The late proterozoic high grade basement of Sri Lanka is divided into three main and one subordinate lithotectonic units namely Highland Complex (HC), Wanni Complex (WC), Vijayan Complex (VC), Kadugannawa Complex (KC).

The most of disasters (Landslides / Cutting failures) happen in Sri Lanka are found in the Highland Complex of Sri Lanka. This Highland Complex occupies the central island as well as most of the south-western part of the island and extends to the north-eastern coast in the form of a narrow belt. It consists of meta-sedimentary rocks, migmatite and meta-igneous rock. The meta-sedimentary rocks are meta-quartzite, marble, Calc silicate, granulites, garnet -silimanite- graphite gneiss, cordierite bearing gneiss, garnet biotite gneiss, garnet quartz-feldspar granulites and gneisses. Over 50% of the complex is made up granitoid origin quartzfeldspathic banded gneisses and charnockitic gneisses tectonically interlayer with metasediments. Recent isotopic studies suggest that the Highland Complex rocks have Nd model ages ranging from 2.0 Ga to 3.0 Ga.

The Johnston Estate Resettlement Site located in central part of Highland Complex in Sri Lanka is the selected location for improving of proper drainage system in order to ensure the safety of residents. The geological observation at the study area reveals;

- The entire site area is located along escarpment slope of composition layers of bedrock.
- Two joint sets with moderately high joint intensity were developed in bedrock within the

- Rock boulders separate along joint planes of bedrock were observed in South direction to the proposed site area.
- Two scars formed under paleo-landslides were observed into South & S-E direction to the site area.
- Debris including large rock boulders were encountered at South & S-E direction to upper part of the proposed site area.

## 6. Hydrology Analysis

Hydrologic analyses must still rely in part on judgment and experience. Use of ArcGIS can be allowed to accommodate more detailed appraisal of the spatial variations in hydrologic parameters than would be feasible using manual procedures.

As per the rasters map of the Johnston Estate initially flow direction model was developed (see Fig 06).

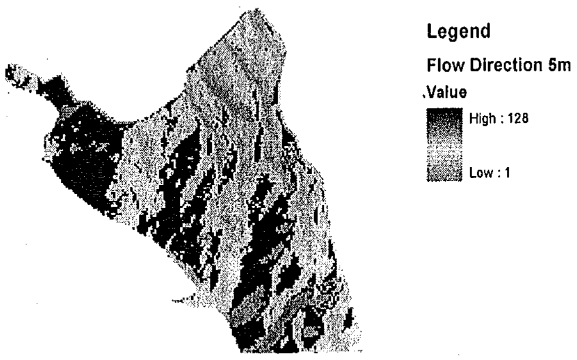


**Fig04**: Flow direction map

Based on the flow direction model the hydrologic analyses are designed to model the convergence of flow across a natural terrain surface at Johnston estate.

For the hydrology analysis, it was assumed that the surface contains sufficient vertical relief that a flow path can be determined. The functions assume that water can flow in from many cells but out through only one cell. According to the assumption, hydrology analysis (flow accumulation) models of Johnston estate are given in Fig: 07 and Fig 08 (a) and (b).

During the design of drainage facilities, Peak discharges are essential. For the hydrological analysis, the discharge can be considered as a hydraulic load as it directly affects the design size of a drainage structure.

Graphical elements of the model describing the location and shape of features are dynamically linked to databases which describe the properties of the features. Cells used for modeling involved mathematical functions and logical operators for flow rate of drains.

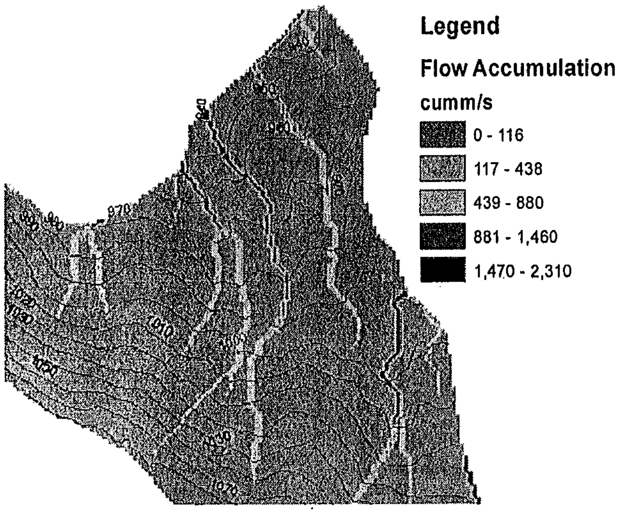


**Fig05:** Hydrology analysis models (2D) of Johnston estate

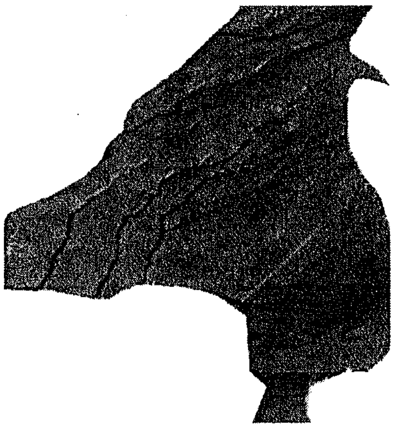

(a)

(b)

**Fig06:** Hydrology analysis models (3D) of Johnston estate (a) with contours (b) without contours

## 7. Design consideration

The design for the sizes of catch drain and the collector drains in the slopes is based on the amount of surface runoff it has to cater. The amount of surface water could be estimated based on the following factors

- Intensity of rainfall
- Catchments area
- Flow accumulation
- Flow directions
- Loss of runoff water

Based on the above model, the catchments area, flow accumulation and flow directions are calculated considering the highest rainfall (257 mm/day) at Johnston estate and assuming all rain became runoff and no loss of water because of interception, evaporation, transpiration, or loss to groundwater. Therefore, actual flow accumulations are calculated considering loss of runoff water. According to the surface and subsurface soil condition and vegetative cover at Johnston Estate the factor of loss of runoff value was determined as 0.25. Flow accumulation from Fig07 and consequent calculated actual flow accumulation are given in following table 1.

**Table 01:** Calculated actual flow accumulation

| Flow Accumulation ($Q_F$) From Fig7 | Accumulation on unit cell ($Q_C$) (m) | $Q_h$ ($m^3$/hour) | $Q_s$ $m^3/s$ |
|---|---|---|---|
| 2,310.00 | 24.74 | 618.41 | 10.31 |
| 1,460.00 | 15.63 | 390.85 | 6.51 |
| 880.00 | 9.42 | 235.58 | 3.93 |
| 438.00 | 4.69 | 117.26 | 1.95 |
| 116.00 | 1.24 | 31.05 | 0.52 |

Where

$$Q_C = Q_F \,.\, Cell_{Area}\,,\; Cell_{Area} = 25\text{m}^2$$

$$Q_{day} = \frac{Q_C}{24}$$

## 8. Design of collection drains, culverts and cascades

Based on the model the design consisted of collector side drains, culverts as well as cascades and they were based on the amount of surface runoff along the slope at the site.

For the drains design, the cross sectional areas of the drains are calculated based on the velocity of flow rate. According to the sandy soil condition at the Johnston estate, selected safe flow velocity is not more than 2m/s. Thus the actual flow accumulation ($Q_L$) and consequent drain size are given in following table 2.

**Table02:** Calculated drain size

| $Q_L$ $m^3/s$ | V m/s | Area $m^2$ | Depth m | Width m |
|---|---|---|---|---|
| 7.73 | 1.93 | 4.00 | 1.5 | 2.7 |
| 4.89 | 1.95 | 2.50 | 1.5 | 1.7 |
| 2.94 | 1.96 | 1.50 | 1.5 | 1.0 |
| 1.47 | 1.47 | 1.00 | 1.5 | 0.7 |
| 0.39 | 0.39 | 1.00 | 1.5 | 0.7 |

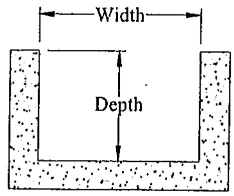


Fig.7 typical section of the drain

Where

V = Velocity (m/s), More than 2m/s

Area = Depth (m) x Width (m)

Surface runoff can be controlled by providing side drains, cascades and culverts without causing erosion and infiltration. A 3D model was built using GIS and drain sizes were estimated using this 3D model and Table 02. Finally it was compared with existing drainage at Johnston Estate and required modifications were done.

Collector drains, cascades and culverts designed based on the hydrological model was compared with the existing natural drainage system. Then it was found that results were matching with the existing drains. Therefore, few changes were introduced and the detailed surface drainage system was proposed without changing natural drainage characteristics of the hill slope.

## 9. Conclusions

The all developed models depend on many parameters such as intensity of rainfall, catchments area and cell size etc., Therefore data collecting, identifying, selecting and calculating procedures are not feasible with manual calculations. Thus, use of GIS model can be allowed to accommodate more detailed appraisal of the spatial variations in hydrologic parameters than manual procedures. Moreover, using accurate factors for analysis can produce accurate result from GIS model than manual procedures.

Therefore, the GIS models appear to be an excellent environment for developing Hydrological model and planning for this type of situations.

## 10. References


Engineering hand book second edition Edited by W.f. CHEN and J.Y. RICHARD LIEW

Engineering hand book by P.N.KANNA

An introduction to geology if Sri Lanka (Ceylon), 2nd edition by P.G COORY, National Museums of Sri Lanka publication, Colombo 340 pp.

Geotechnical engineering Investigation handbook Second Edition by ROY E. HUNT

System of GIS-based hydrologic and hydraulic applications for highway engineering by FRANCISCO OLIVERA and DAVID MAIDMENT center for transportation research bureau of engineering research the University of Texas at Austin (REPORT 1738-S)